CHAPTER V

RESULTS AND DISCUSSION

In this chapter are divided into two sections. Section 5.1 is described characteristics of cobalt (Co) dispered on mixed nano-SiO_2/ZrO_2 supports. Section 5.2 differences in characteristics and catalytic activity toward CO hydrogenation of Co catalysts dispersed on various micron- and nanoscale mixed SiO_2-ZrO_2 supports.

5.1 Various nanoscale mixed SiO_2/ZrO_2 supports

5.1.1 BET surface area

Table 5.1 BET surface area measurement of samples in nano scale.

Supports	BET surface area (m^2/g)	Catalyst samples	BET surface area (m^2/g)
SiO_2	297.60	Co/SiO_2	262.80
Si-40-Zr-60	159.61	Co/Si-40-Zr-60	141.04
ZrO_2	24.75	Co/ZrO_2	18.05

5.1.2 X-ray diffraction (XRD)

XRD patterns of the mixed nano-SiO_2/ZrO_2 supports before impregnation with the cobalt precursor are shown in **Figure 5.1**. It was observed that the pure SiO_2 exhibited only a broad XRD peak assigning to the conventional amorphous silica. The pure ZrO_2 exhibited the XRD peaks at 30°, 35°, 50°, and 60° assigning to the ZrO_2 in tetragonal phase. Besides, the XRD peaks at 29°, 32°, and 55° were also detected indicating the ZrO_2 in monoclinic phase. XRD patterns of the mixed supports containing different weight ratios of SiO_2/ZrO_2 revealed the combination of SiO_2/ZrO_2 supports based on their content. After impregnation with the cobalt precursor, the catalyst samples were dried and calcined. The XRD patterns of the mixed SiO_2/ ZrO_2 - supported Co catalyst are shown in **Figure 5.2**. Besides the

observation of the characteristic peaks of the supports as shown in **Figure 5.1**, all calcined samples exhibited XRD peaks at 31° (weak), 36° (strong), and 65° (weak), which were assigned to the presence of Co_3O_4. This indicated that the Co_3O_4 formed was highly dispersed.

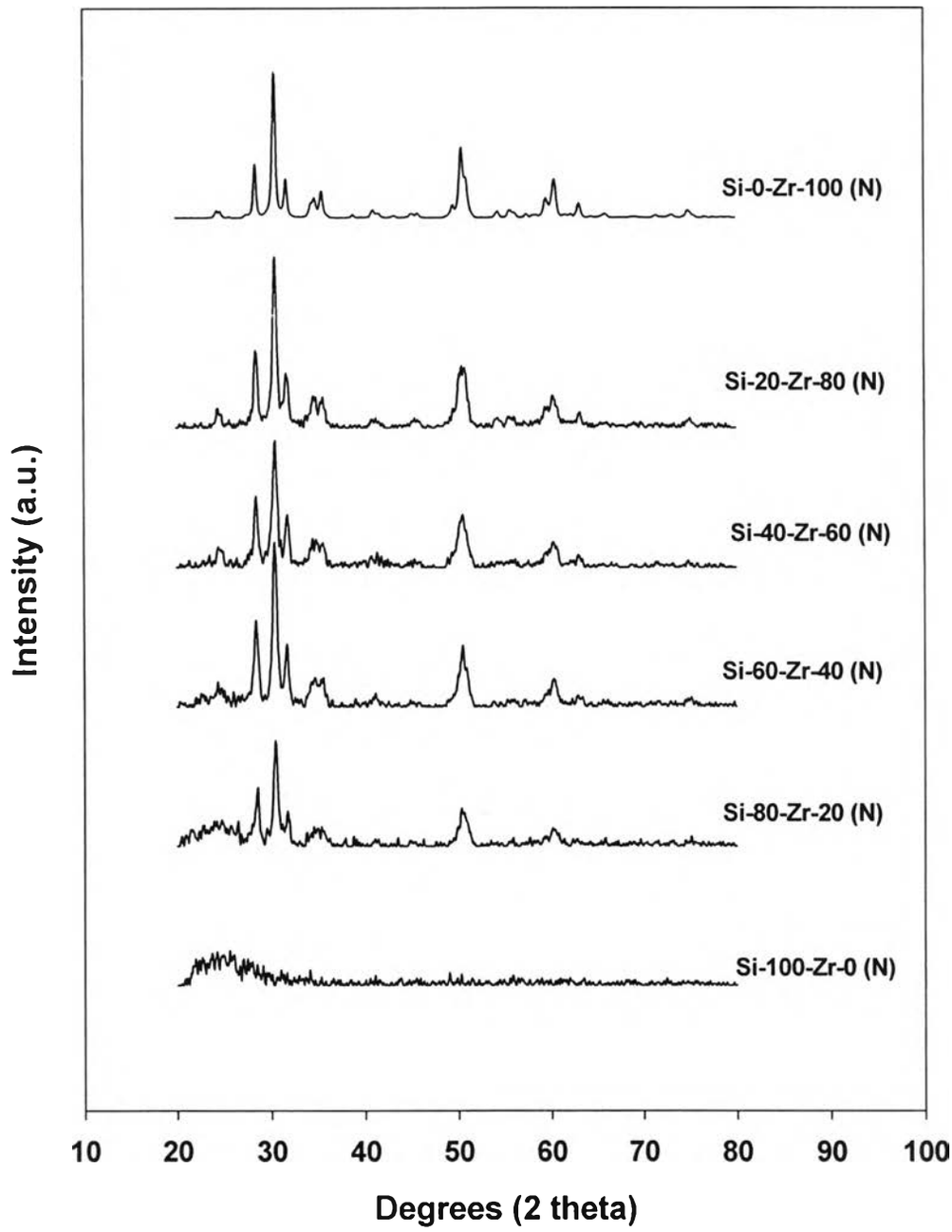

Figure 5.1 XRD patterns of the mixed nano-SiO_2/ZrO_2 supports before impregnation with the cobalt precursor.

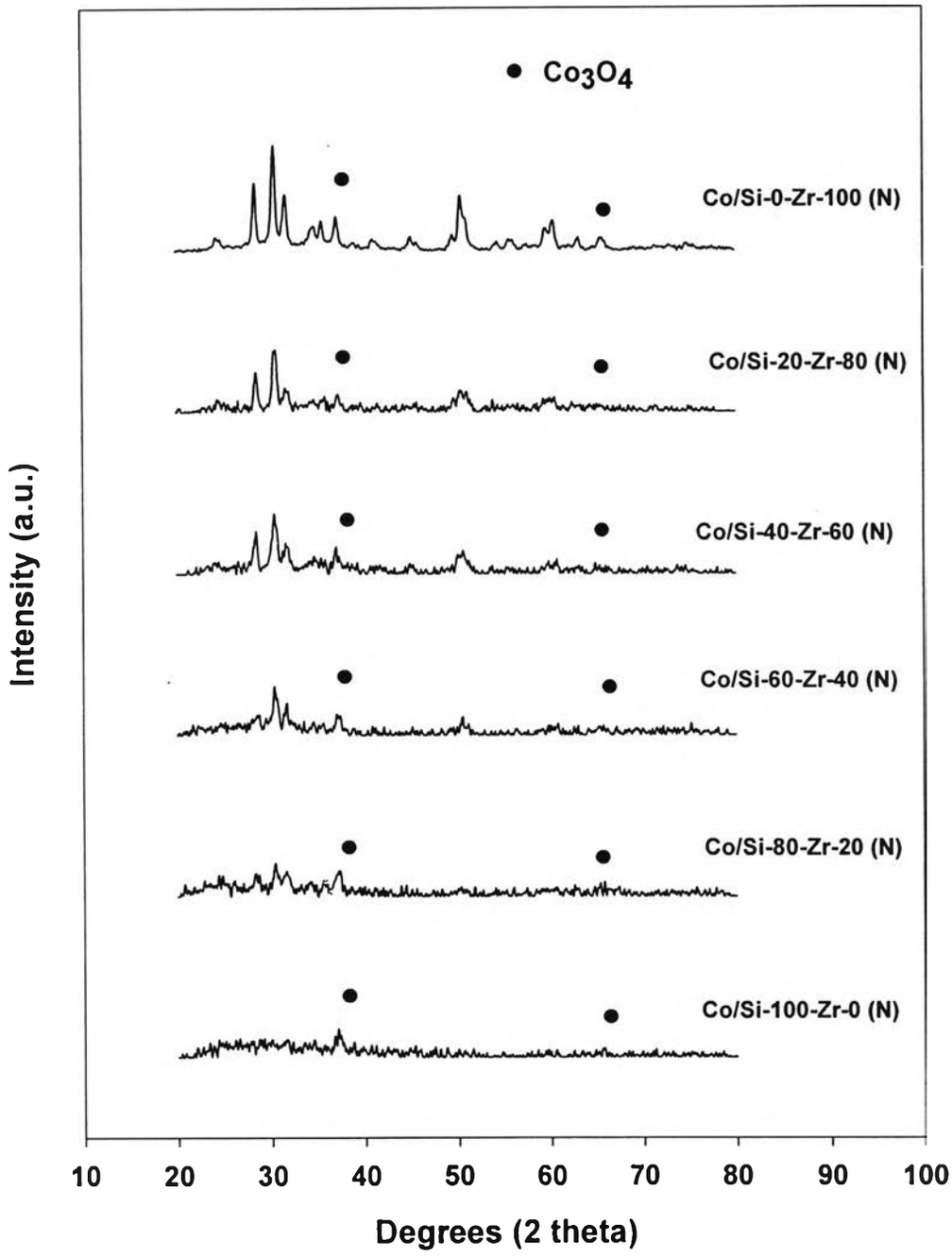

Figure 5.2 XRD patterns of the mixed nano- SiO_2/ZrO_2-supported Co catalyst.

5.1.3 Scanning electron microscopy (SEM) and Energy dispersive X-ray spectroscopy (EDX)

SEM and EDX were also conducted in order to study the morphologies and elemental distribution of the samples, respectively. In general, there was no significant change in morphologies and elemental distribution of all catalyst samples after calcination. A typical SEM micrograph and EDX mapping for mixed nano-SiO_2/ZrO_2 supports before impregnation with the cobalt precursor are illustrated in **Figure 5.3-5.6**. The mixed SiO_2/ZrO_2-supported Co catalyst sample are illustrated in **Figure 5.7-5.12**. It can be seen that ZrO_2 was located on the outer surface of SiO_2. It appeared that the distribution of Co was well on the surface of the support.

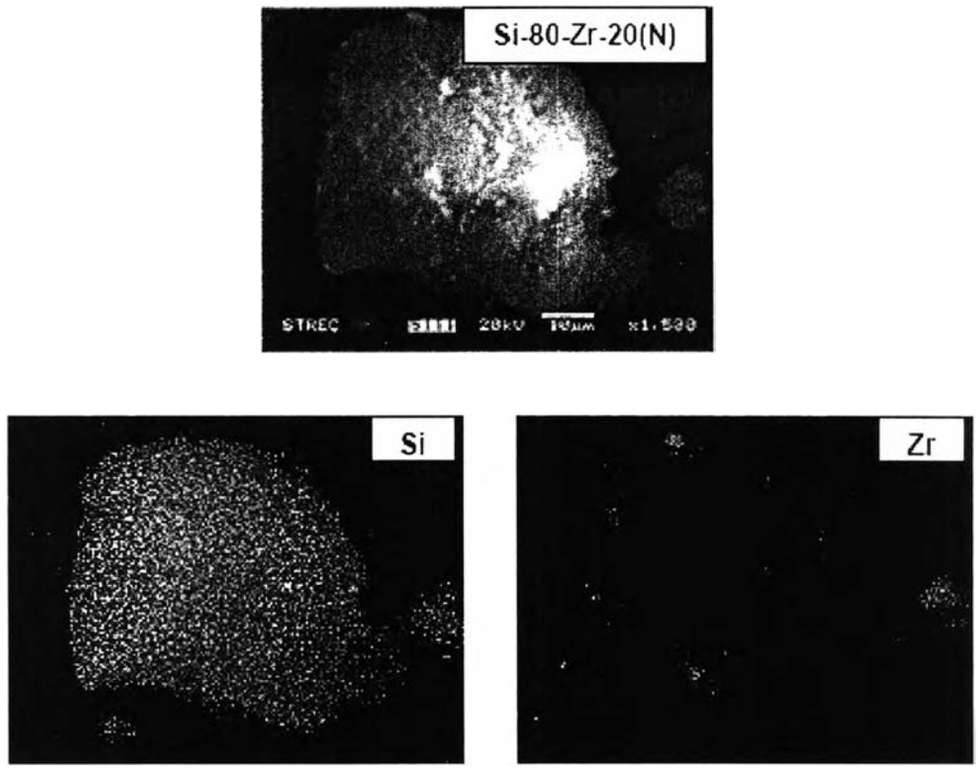

Figure 5.3 SEM micrograph and EDX mapping for Si-80-Zr-20 catalyst granule.

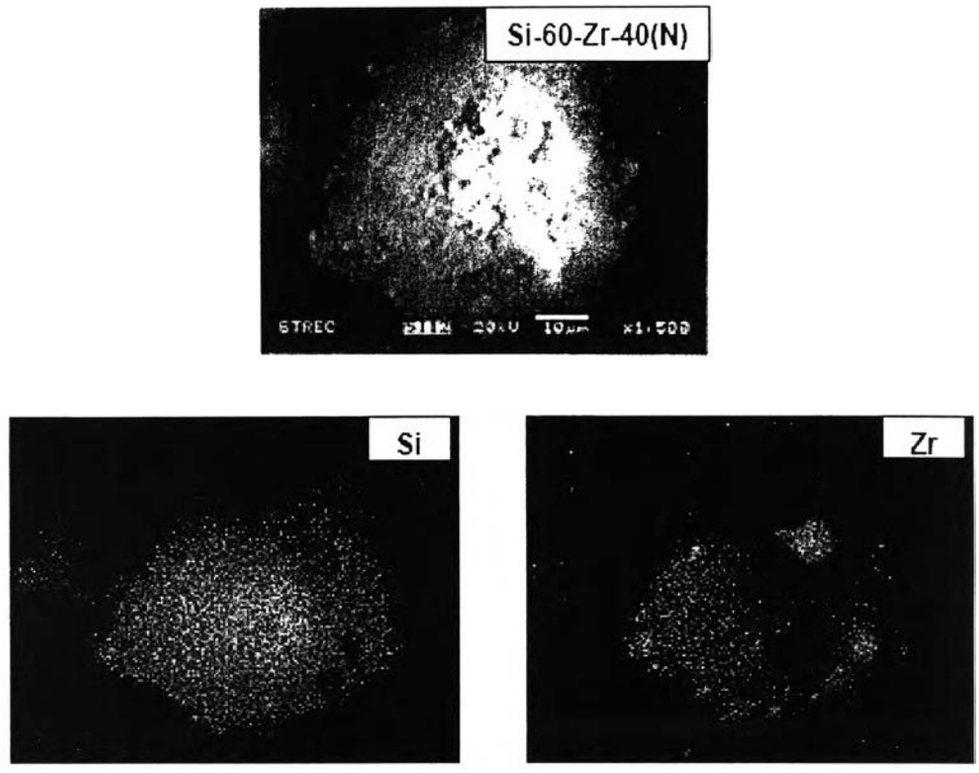

Figure 5.4 SEM micrograph and EDX mapping for Si-60-Zr-40 catalyst granule.

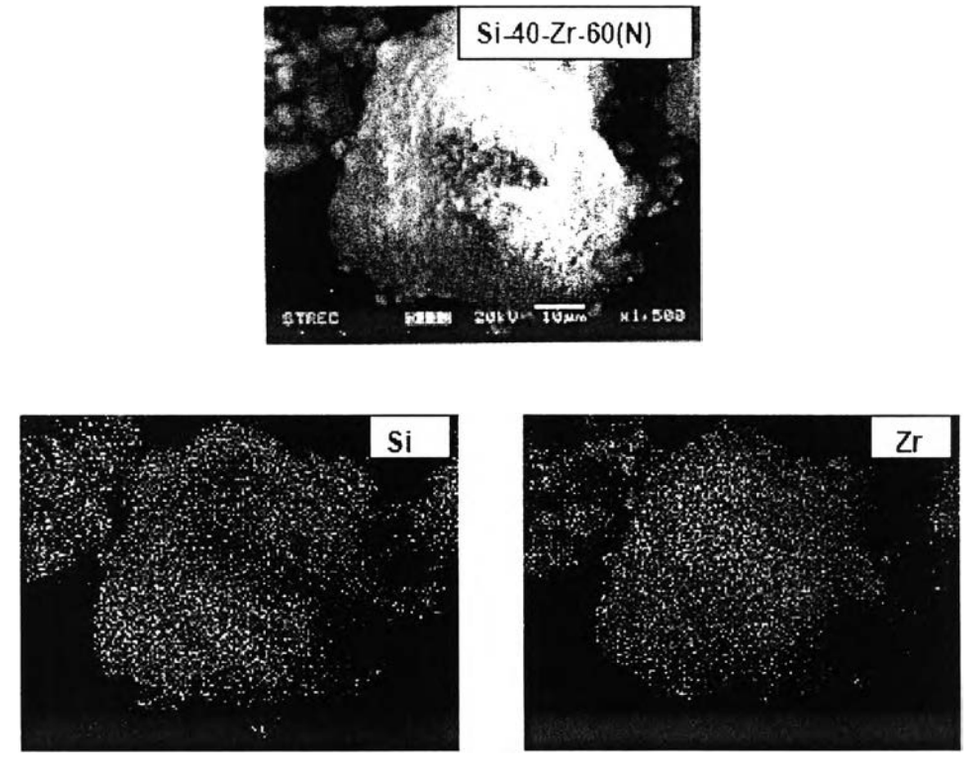

Figure 5.5 SEM micrograph and EDX mapping for Si-40-Zr-60 catalyst granule.

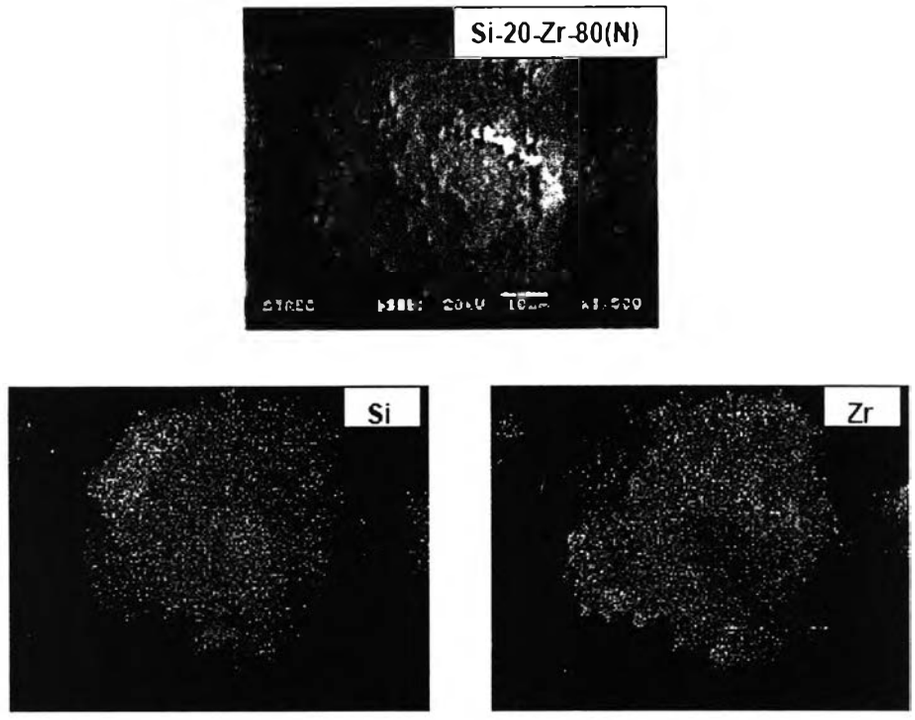

Figure 5.6 SEM micrograph and EDX mapping for Si-20-Zr-80 catalyst granule.

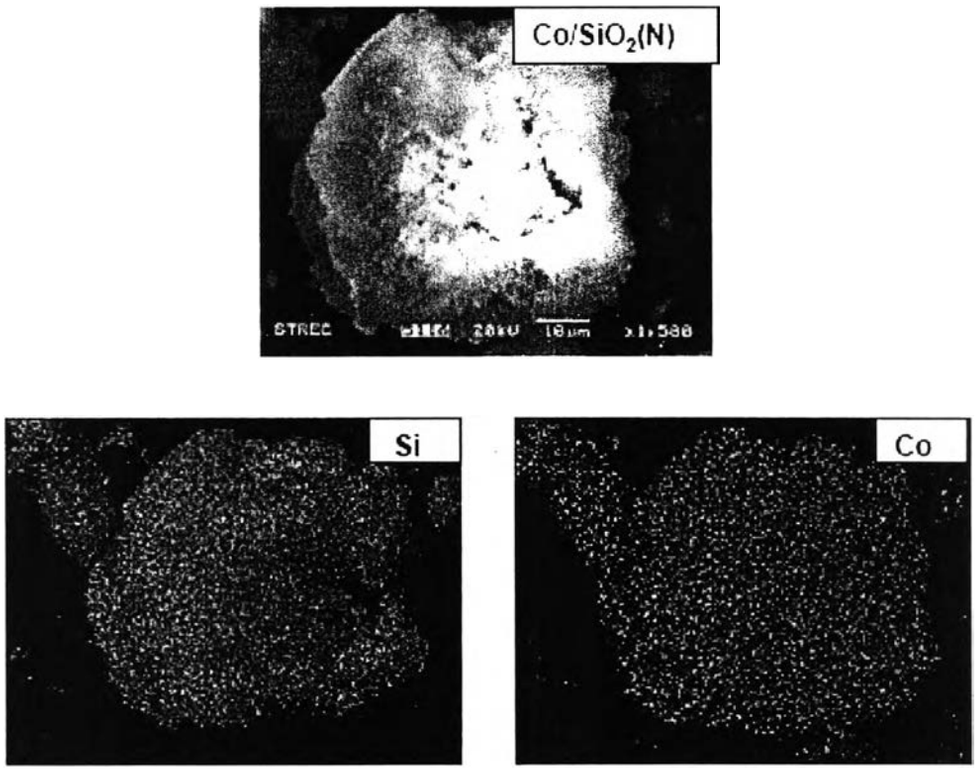

Figure 5.7 SEM micrograph and EDX mapping for Co/SiO_2 catalyst granule.

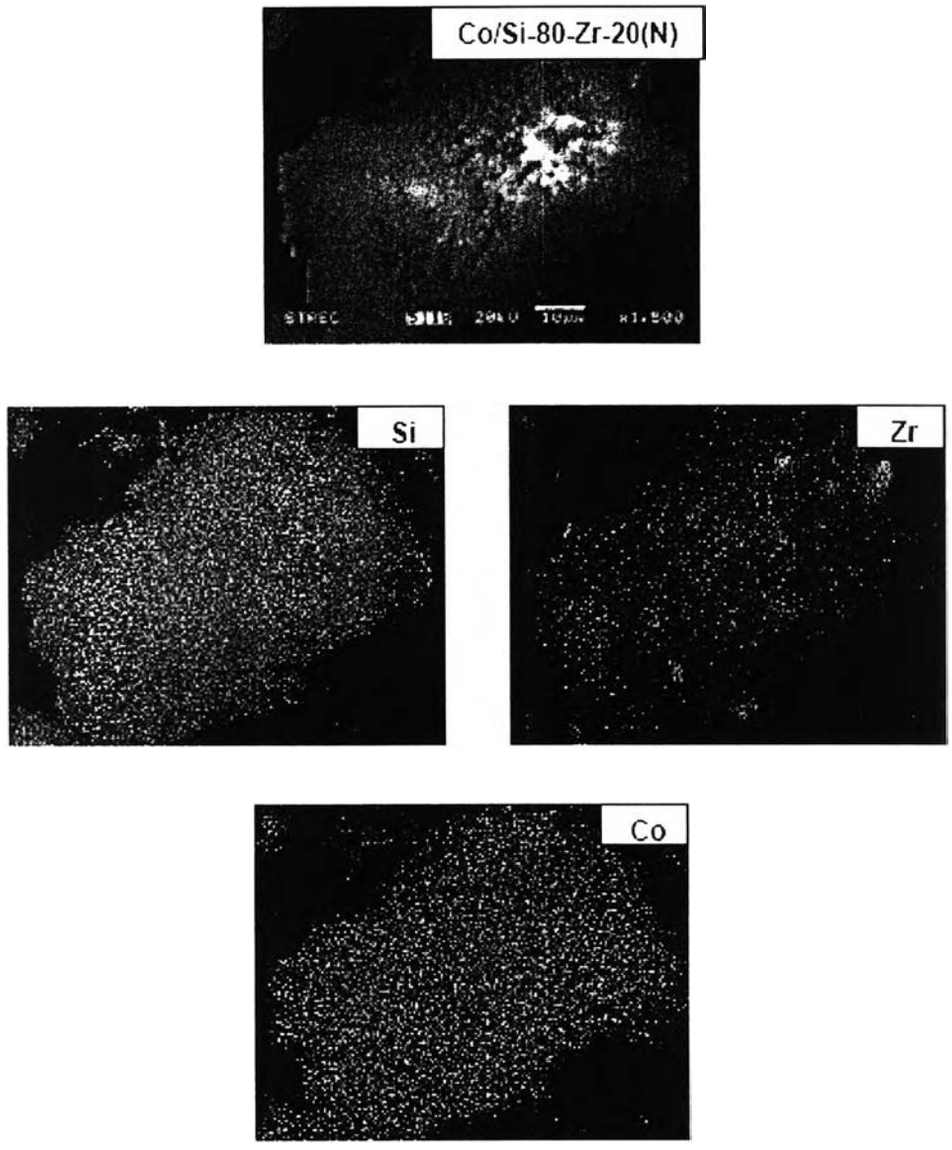

Figure 5.8 SEM micrograph and EDX mapping for Co/Si-80-Zr-20 catalyst granule.

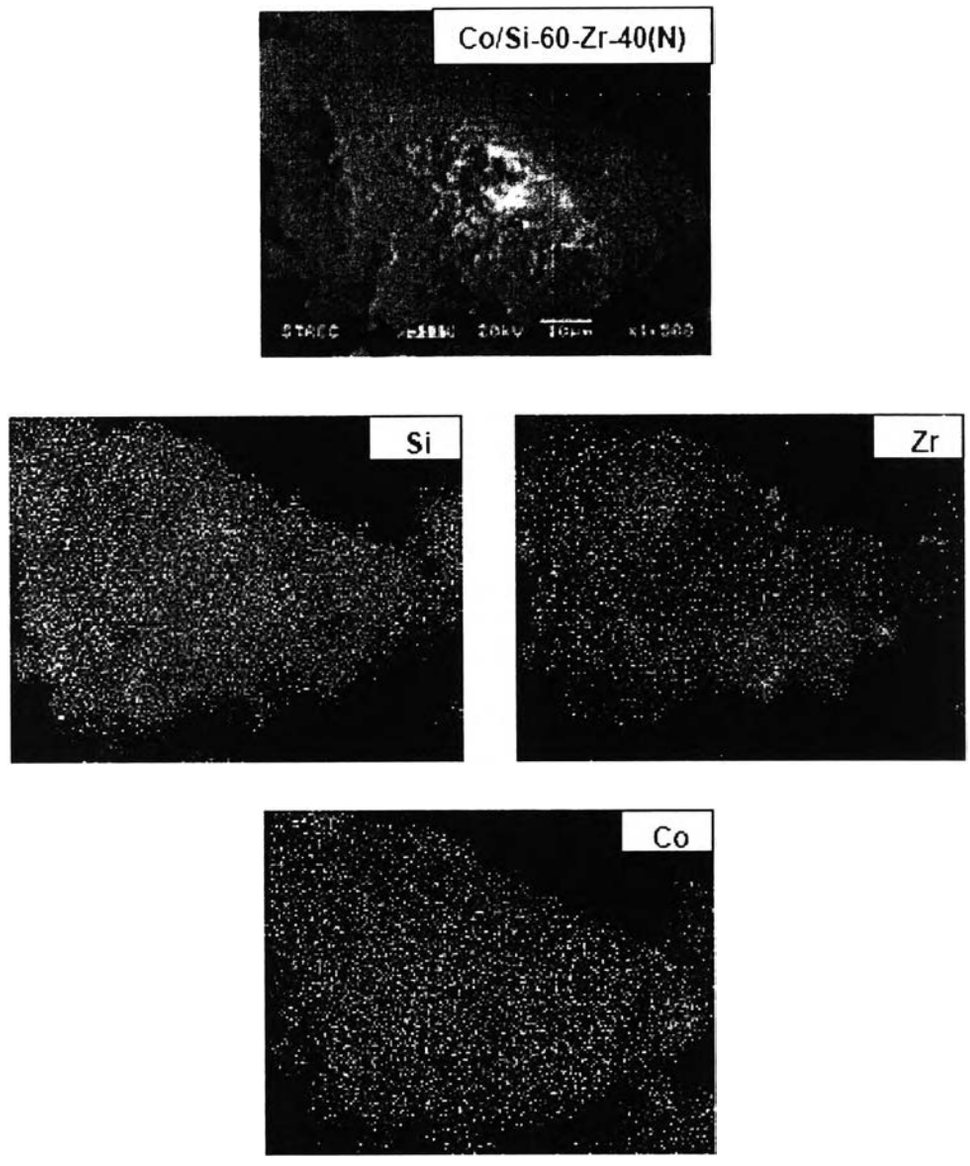

Figure 5.9 SEM micrograph and EDX mapping for Co/Si-60-Zr-40 catalyst granule.

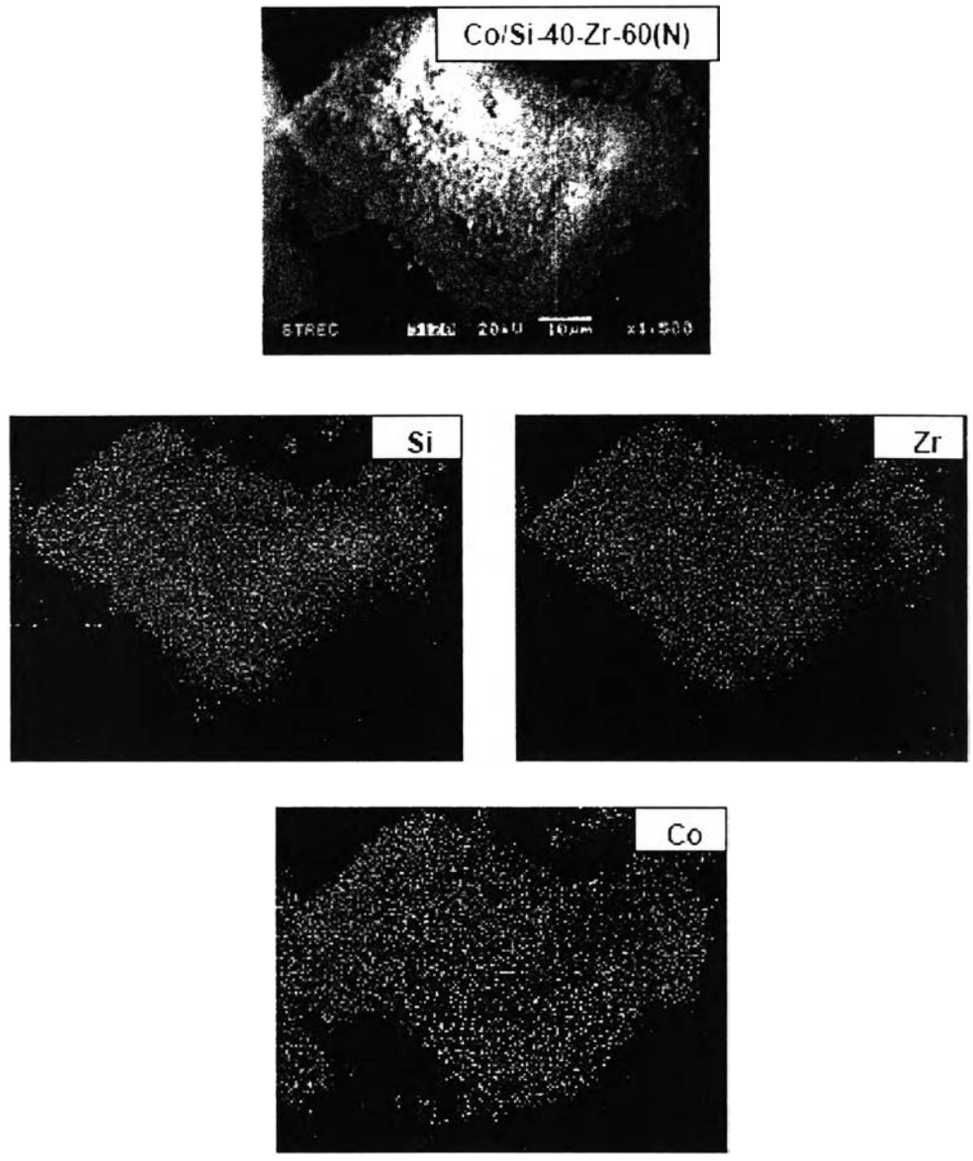

Figure 5.10 SEM micrograph and EDX mapping for Co/Si-40-Zr-60 catalyst granule.

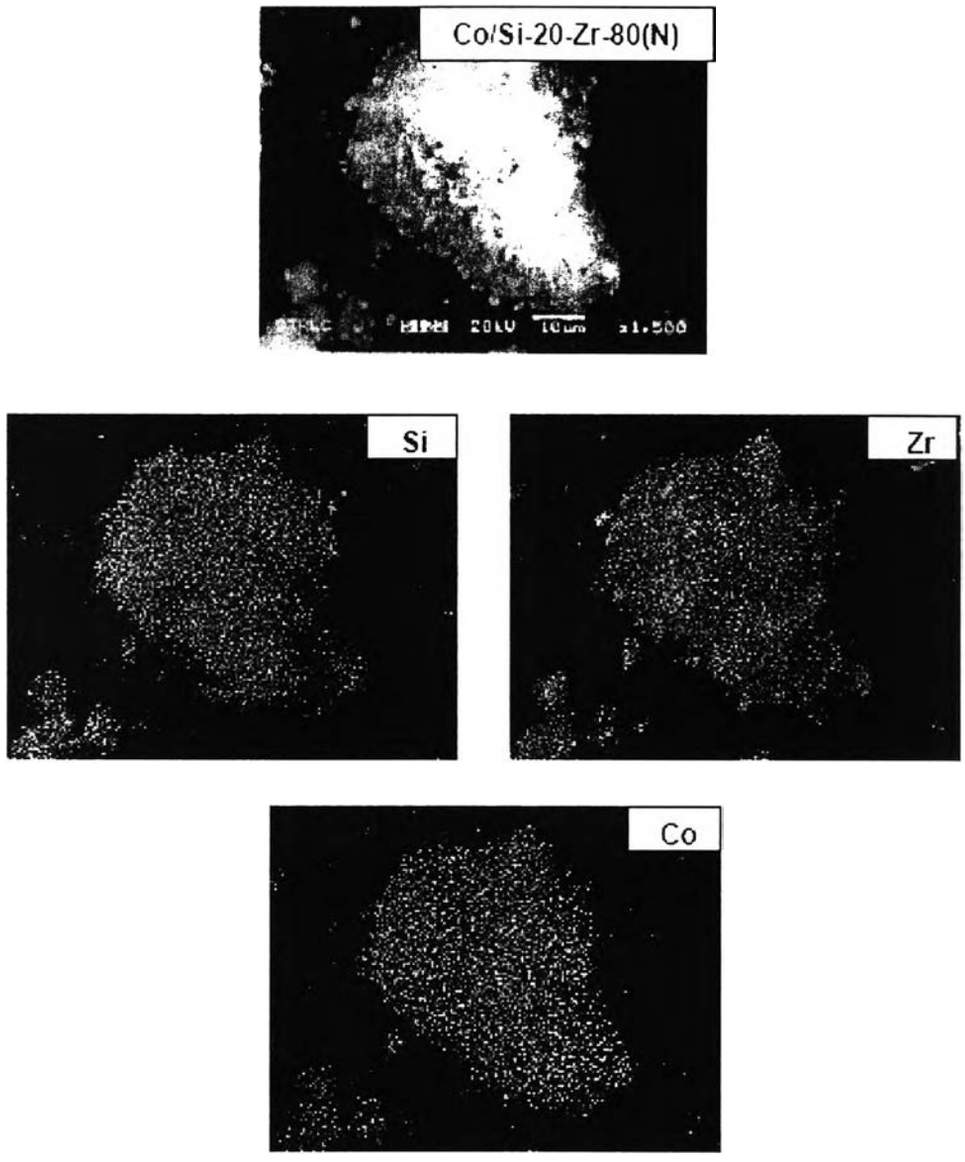

Figure 5.11 SEM micrograph and EDX mapping for Co/Si-20-Zr-80 catalyst granule.

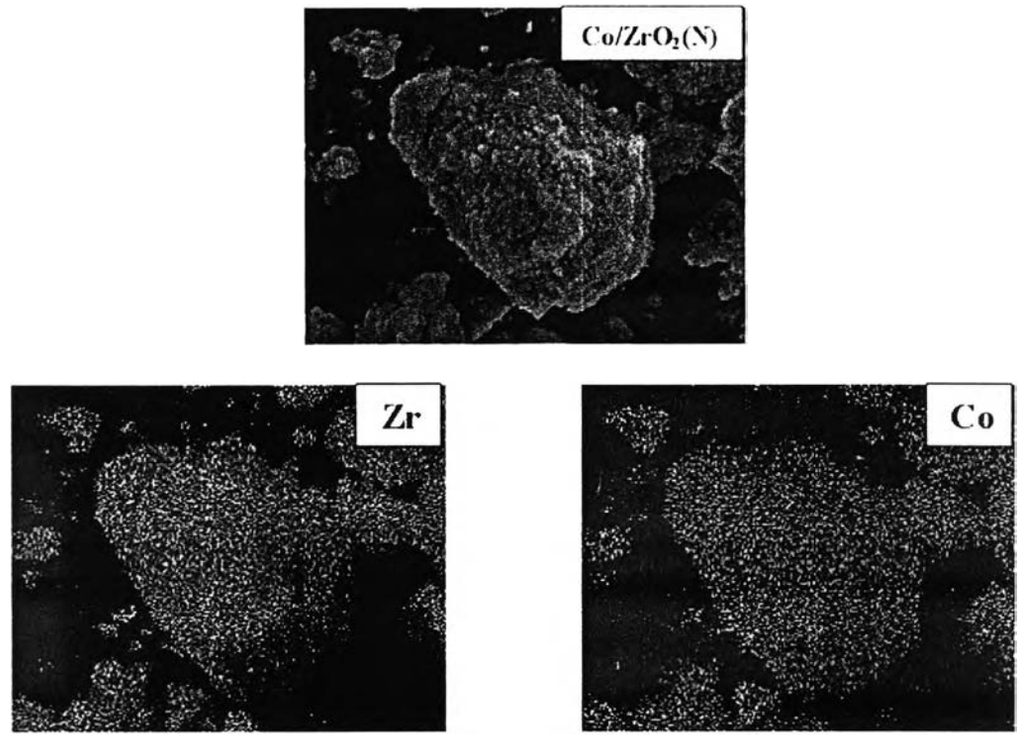

Figure 5.12 SEM micrograph and EDX mapping for Co/ZrO_2 catalyst granule.

5.1.4 Transmission Electron Microscopy (TEM)

In order to determine the dispersion of cobalt oxide species on the various mixed supports, a more powerful technique such as TEM was applied to all samples. First, TEM micrographs of the mixed supports were collected and the typical TEM micrographs of the nano-SiO_2, the nano-ZrO_2 and the mixed nano-SiO_2/ZrO_2 (Si-40-Zr-60) supports are shown in **Figure 5.13**. As seen, the nano-SiO_2 appeared in smaller particle than that of the nano-ZrO_2. The mixed supports exhibited the combination between both supports present. Besides, the TEM micrographs for all cobalt dispersed on the various supports are shown in **Figure 5.14**. However, considering the morphologies for the cobalt oxide species dispersed on they support, they could not differentiated between those and the supports. This was suggested that the morphologies of cobalt oxide species were essentially similar with those of the various supports indicating the more uniform of cobalt oxide species on the supports.

On the other hand, it revealed that the nano-size of cobalt oxide species could be achieved with the nano-sized supports. In addition, the cobalt oxide species were also located and distributed side by side with the supports showing good distribution of the species. There was no significant change based on different compositions of the support. It should be noted that the highly dispersed form of cobalt oxide species could not guarantee the large number of reduced cobalt metal surface atoms, which is related to the overall activity of the catalysts during CO hydrogenation reaction (B. Jongsomjit *et al.*, 2005). In addition, with the highly dispersed form of cobalt oxide species, the interaction of those with the specified supports has to be essentially considered. Therefore, the temperature-programmed reduction on the calcined samples needs to be performed in order to give a better understanding according to such a reduction behaviors.

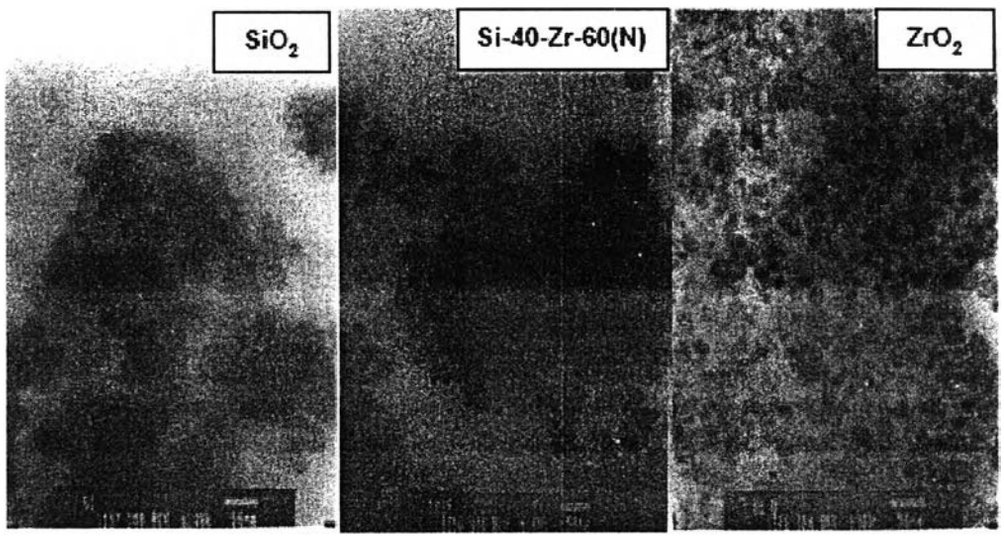

Figure 5.13 TEM micrographs of the nano-SiO_2, the nano-ZrO_2 and the mixed nano-SiO_2/ZrO_2 supports.

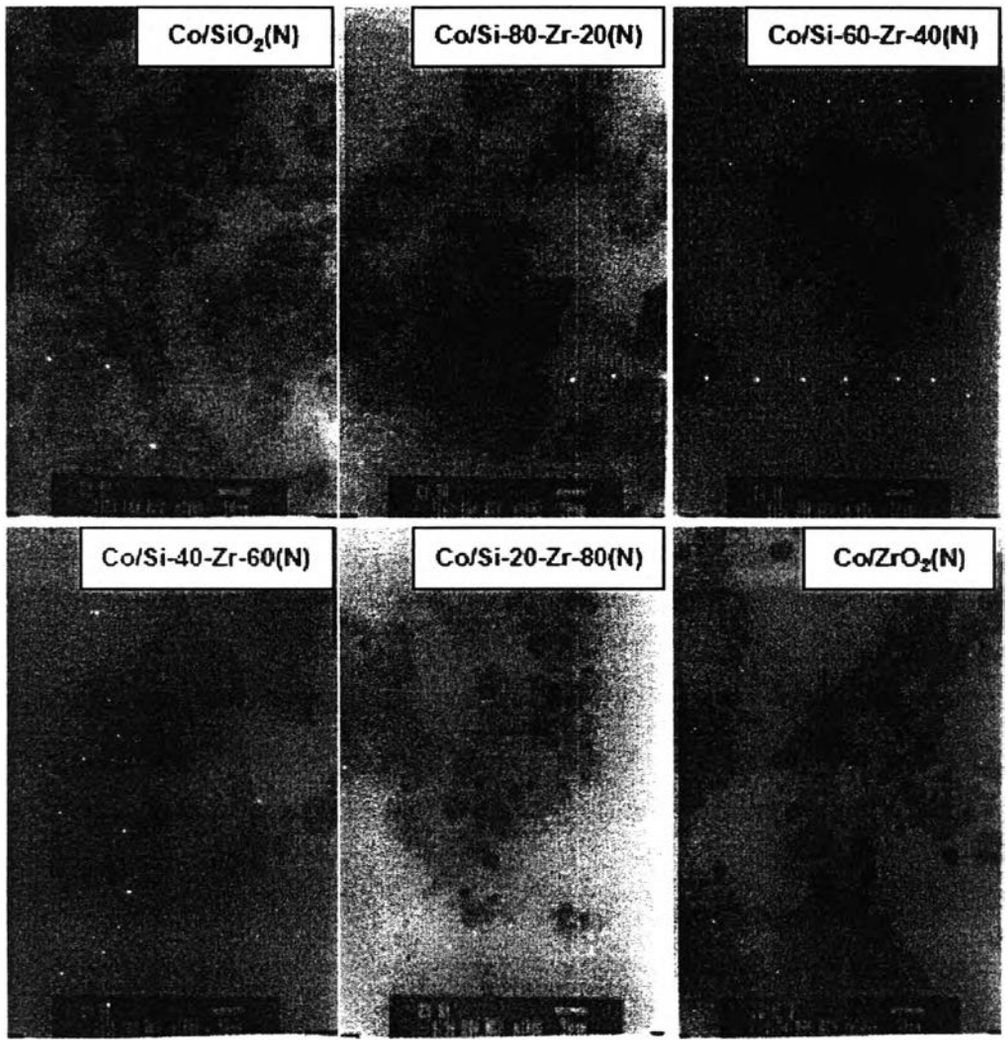

Figure 5.14 TEM micrographs for all cobalt dispersed on the various supports.

5.1.5 Temperature programmed reduction (TPR)

TPR was performed in order to determine the reduction behaviors of samples. The TPR profiles for all samples are shown in **Figure 5.15**. It was found that there was only one reduction peak, however, at different reduction temperatures for all calcined samples. The one reduction peak can be assigned to the overlap of two-step reduction of Co_3O_4 to CoO and then to Co metal (G.Jacobs *et al.*, 2002; J.L.Li *et al.*, 2002)]. Upon the TPR conditions, the two-step reduction may or may not be observed. Based on the TPR profiles, it indicated that Co oxides dispersed on the pure SiO_2 and ZrO_2 exhibited higher maximum reduction temperatures than those on the mixed SiO_2/ZrO_2 supports. It was suggested that using the mixed SiO_2/ZrO_2 supports could result in lowering the reduction temperature of Co oxides.

Table 5.2 Initial, final and maximum temperature from TPR profiles for the mixed nano-SiO_2-ZrO_2-supported Cobalt catalyst.

Catalyst samples	Temperature (°C)		
	Initial	Final	Maximum
Co/SiO_2 (N)	320	580	460
Co/Si-80-Zr-20 (N)	260	595	440
Co/Si-60-Zr-40 (N)	275	595	455
Co/Si-40-Zr-60 (N)	290	590	450
Co/Si-20-Zr-80 (N)	295	600	445
Co/ZrO_2(N)	265	620	470

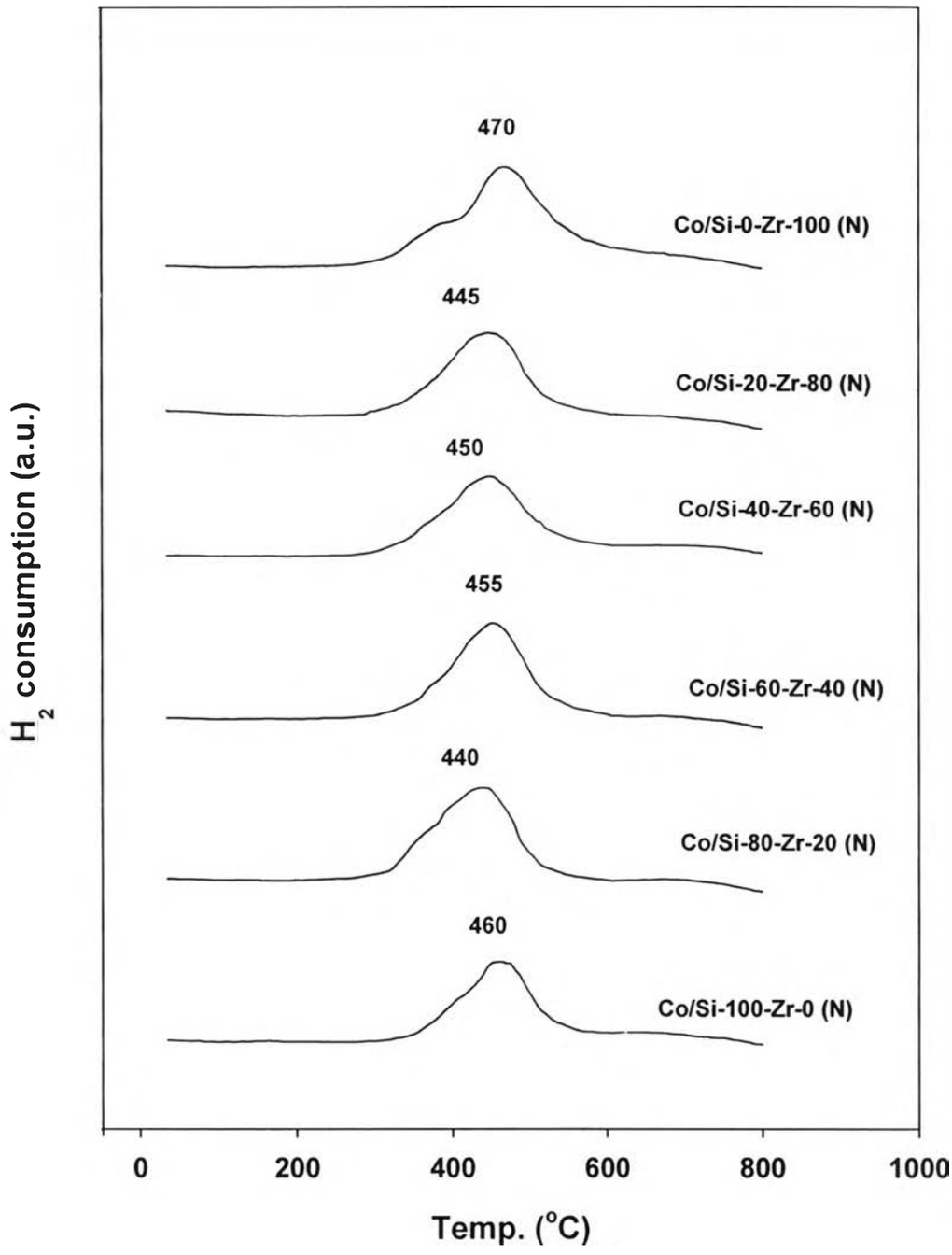

Figure 5.15 TPR profiles for the mixed nano- SiO_2/ZrO_2-supported Co catalyst.

5.1.6 H_2 chemisorption

H_2 chemisorption was performed in order to measure the number of reduced cobalt metal surface atoms, which is related to the overall activity during CO hydrogenation. The resulted H_2 chemisorption is illustrated in **Table 5.3**. The amounts of H_2 adsorbed on the catalytic phase were in the range of 1.21 to 6.12 μmol/g of sample. It was found that the number of the reduced cobalt metal surface atoms was the largest for the cobalt dispersed on the mixed nano-SiO_2-ZrO_2 (Co/Si-20-Zr-80) support. It seemed that the use of mixed nano-SiO_2-ZrO_2 support consisting of lower amounts of nano-SiO_2.

5.1.7 Reaction study in CO hydrogenation

In order to determine the catalytic behavior of samples, CO hydrogenation (H_2/CO = 10/1) was performed to determine the product selectivity of samples. As expected, the reaction rate was in accordance with the H_2 chemisorption results as mentioned before. The selectivity of products is also shown in **Table 5.3**. In fact, it appeared that the presence of nano-ZrO_2 in the mixed supports could result in more amounts of long chain hydrocarbons. It is known that CO hydrogenation is a kind of polymerization reactions where insertion of the $-CH_2-$ (methylene group) occurs through the active center. Thus, the product distribution strongly depends on the nature of active centers, rate of propagation, and rate of termination. Obviously, the termination of chain growth occurs and is recognized as the chain growth probability. Based on product selectivity found here, it can be concluded that the presence of the nano-ZrO_2 in the mixed supports apparently enhanced the chain growth probability. As a matter of fact, it resulted in the observation of longer chain hydrocarbons even at the specified methanation condition where the high ratio of H_2/CO (10/1) was applied. Based on using the pure nano-ZrO_2 as a support, the similar trend regarding to the effect of nano-ZrO_2 on the chain growth probability was also observed.

Table 5.3 Results of H_2 chemisorption and selectivity to products

Samples	Total H_2 chemisorption (μmol/g cat)	Selectivity (%) C_1 compound	C_2-C_4 compound
Co/SiO_2 (N)	1.21	99.5	0.5
Co/Si-80-Zr-20 (N)	1.26	98.7	1.3
Co/Si-60-Zr-40 (N)	2.44	98.0	2.0
Co/Si-40-Zr-60 (N)	3.90	99.1	0.9
Co/Si-20-Zr-80 (N)	6.12	99.1	0.9
Co/ZrO_2(N)	2.01	96.3	3.7

5.2 various micron- and nano scale mixed SiO_2-ZrO_2 supports.

5.2.1 BET surface area

Table 5.4 BET surface area measurement of samples in micron and nano scale.

Supports	BET surface area (m^2/g)	Catalyst samples	BET surface area (m^2/g)
SiO_2 (M)	154.15	Co/SiO_2 (M)	132.60
Si-40-Zr-60 M)	77.12	Co/Si-40-Zr-60 (M)	57.29
ZrO_2 (M)	2.90	Co/ZrO_2 (M)	0.95
SiO_2 (N)	297.60	Co/SiO_2 (N)	262.80
Si-40-Zr-60 (N)	159.61	Co/Si-40-Zr-60 (N)	141.04
ZrO_2 (N)	24.75	Co/ZrO_2 (N)	18.05

5.2.2 X-ray diffraction (XRD)

XRD was performed in order to determine the bulk crystalline phases of the supports and catalysts. It can be observed that the XRD patterns for pure micron- and nanoscale SiO_2 exhibited only a broad XRD peak assigning to the conventional amorphous silica. The pure micron- and nanoscale ZrO_2 showed the strong XRD peaks at 29° and 32° assigning to the ZrO_2 in the monoclinic phase. In addition, the strong XRD peaks at 30°, 50°, and 60° were detected for the nanoscale ZrO_2 indicating the ZrO_2 in the tetragonal phase. The XRD patterns of the mixed support containing different weight ratios of the micron- and nanoscale SiO_2-ZrO_2 only revealed the combination of SiO_2 and ZrO_2 with corresponding to their contents in the mixed supports. After impregnation of the support with the cobalt precursor, catalyst samples were dried and calcined. Besides the observation of the characteristic peaks of the supports as mentioned before, all calcined samples exhibited XRD peaks at 31° (weak), 36° (strong), and 65° (weak) indicating the presence of Co_3O_4. No other forms of Co oxide species can be detected by XRD measurement. XRD patterns of the mixed micron- SiO_2/ZrO_2 supports before impregnation with the cobalt precursor are shown in **Figure 5.16**. The typical XRD patterns for Co dispersed on various supports are shown in **Figure 5.17**.

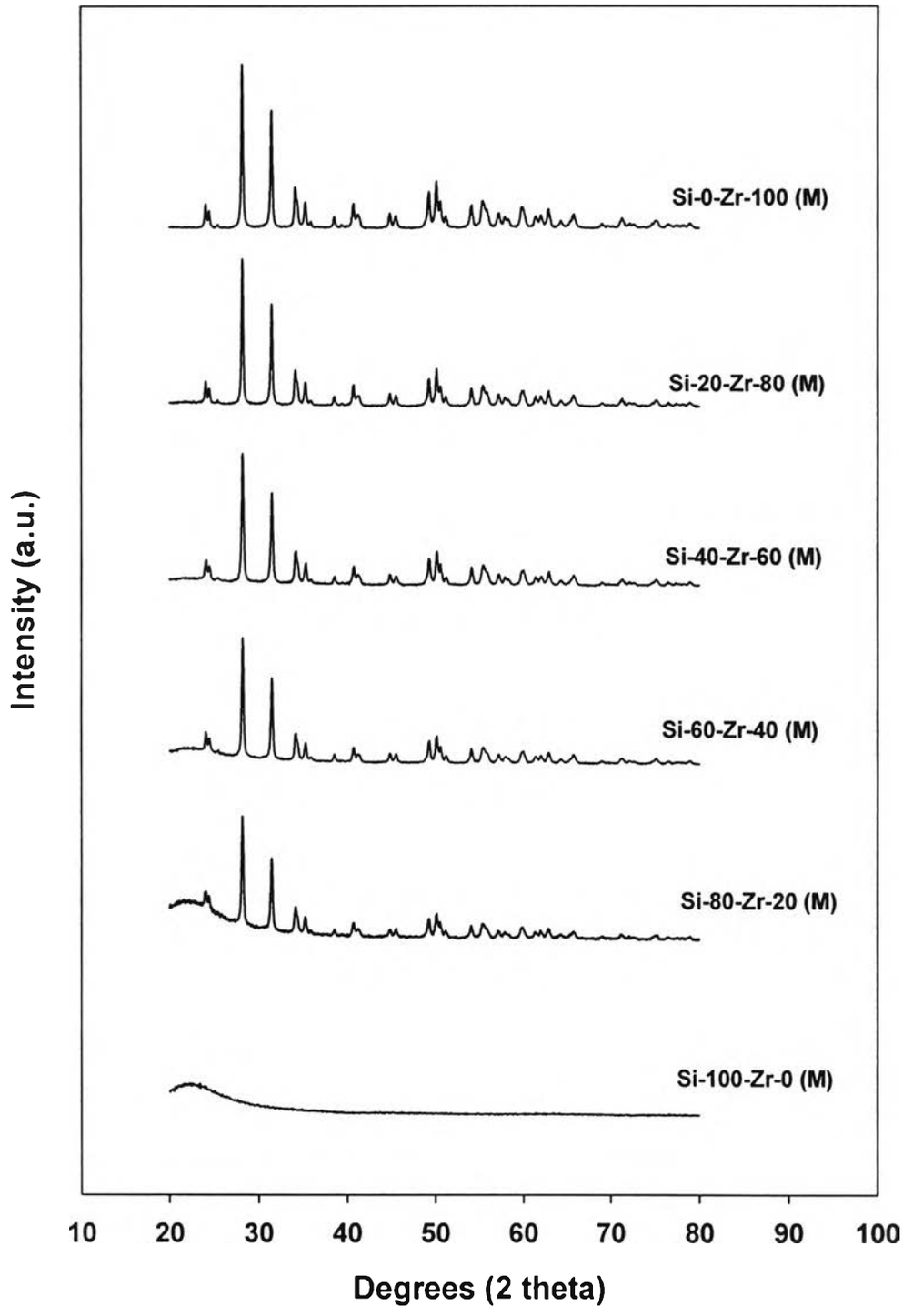

Figure 5.16 XRD patterns of the mixed micron-SiO_2/ZrO_2 supports before impregnation with the cobalt precursor.

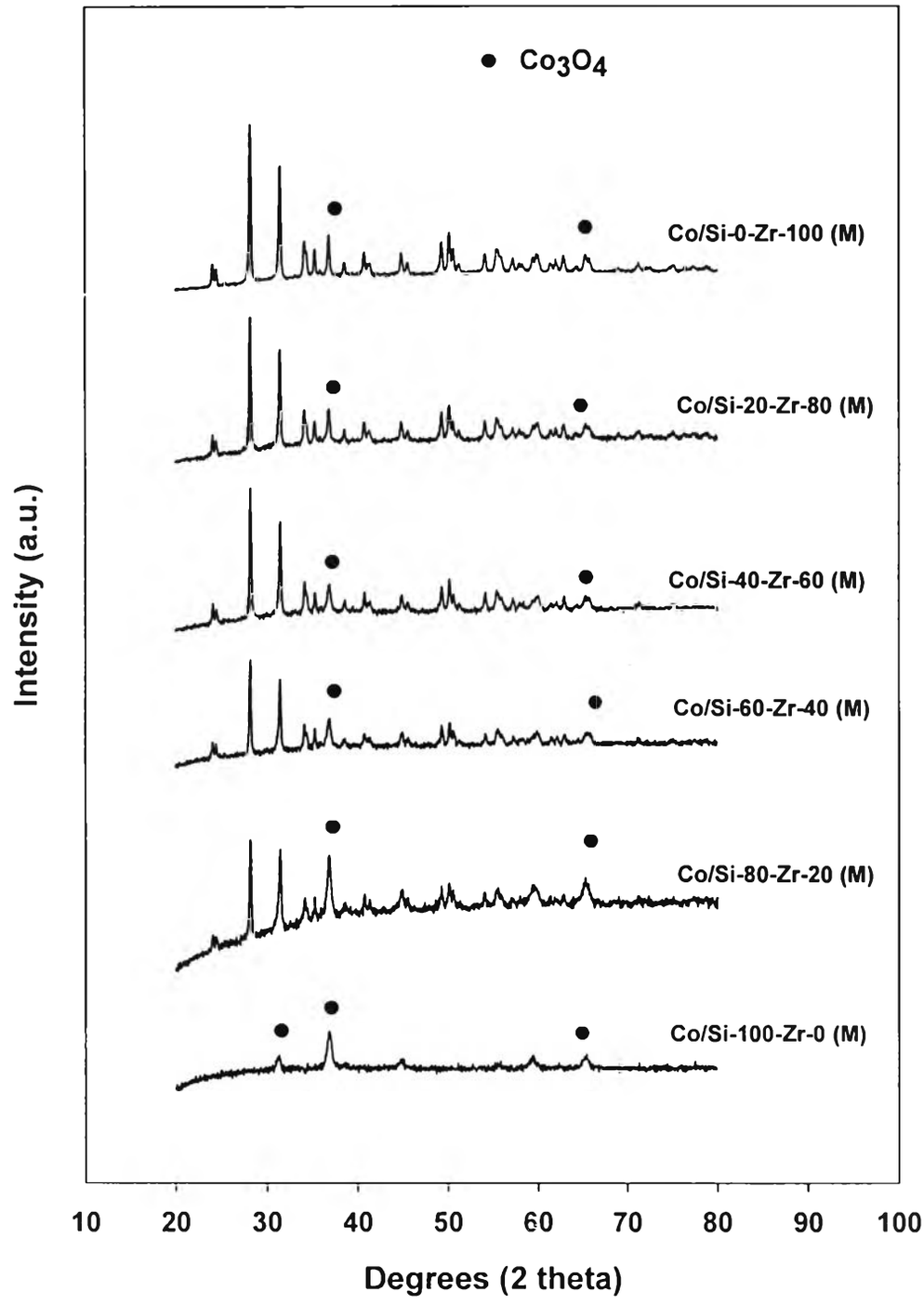

Figure 5.17 XRD patterns of the mixed micron -SiO_2/ZrO_2-supported Co catalyst.

5.2.3 Scanning electron microscopy (SEM) and Energy dispersive X-ray spectroscopy (EDX)

SEM and EDX were also conducted in order to study the morphologies and elemental distribution of the samples, respectively. Apparently, SEM micrographs and EDX mapping exhibited similar trends of morphologies and elemental (Co, Si, Zr, and O) distribution. The typical SEM micrograph along with the EDX mapping (for Si, Zr, and O) of the mixed SiO_2-ZrO_2 support are illustrated in **Figure 5.18-5.21** for Si-80-Zr-20, Si-60-Zr-40, Si-40-Zr-60, and Si-20-Zr-80 supports. The mixed SiO_2-ZrO_2-supported cobalt catalyst (for Co, Si, Zr, and O) are illustrated in **Figure 5.22-5.27** for Co/SiO2, Co/Si-80-Zr-20, Co/Si-60-Zr-40, Co/Si-40-Zr-60, Co/Si-20-Zr-80, and Co/ZrO_2 samples, respectively, indicating the external surface of the sample granule. It can be seen that the cobalt oxide species were well distributed (shown on EDX mapping) all over the sample granule.

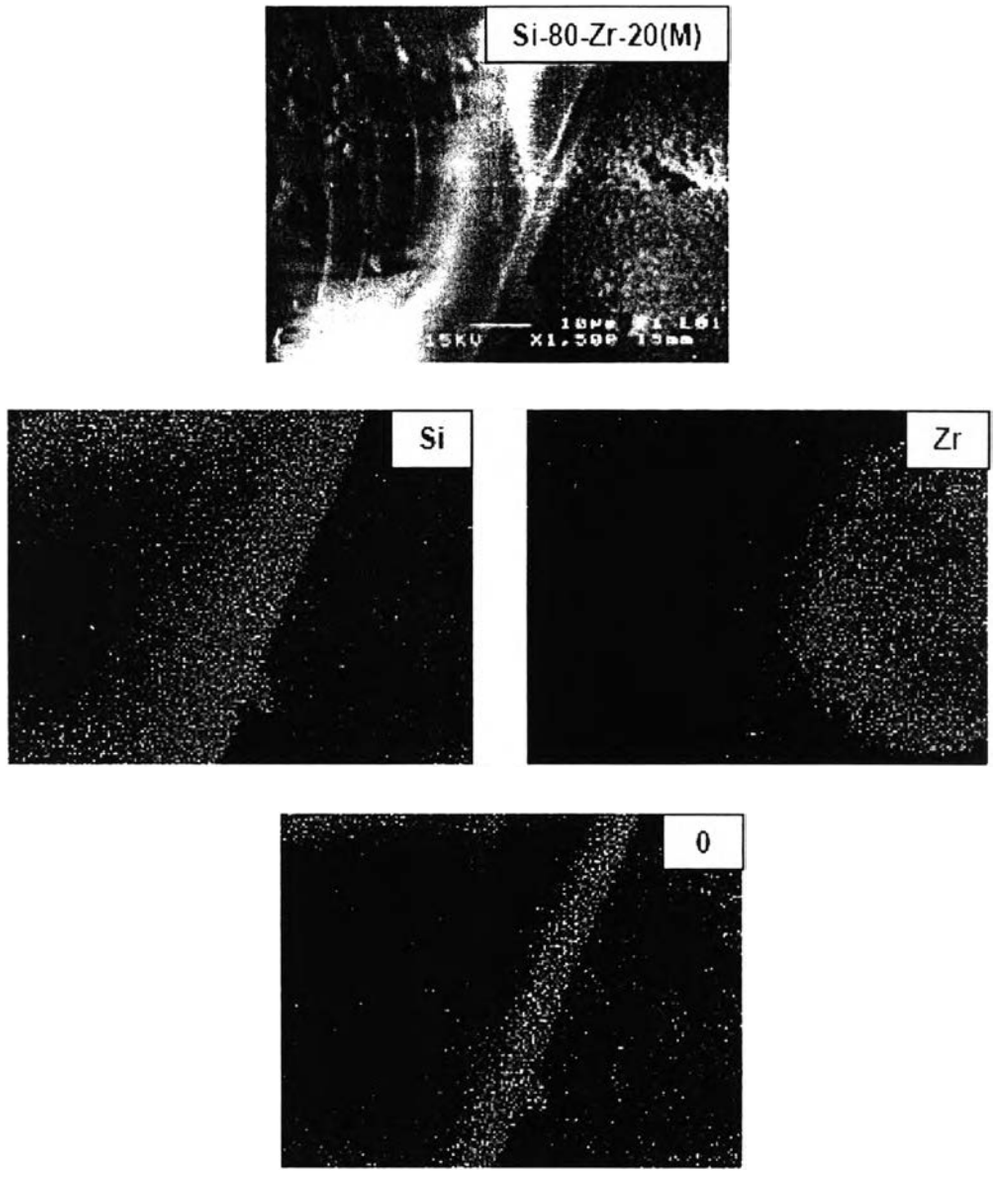

Figure 5.18 SEM micrograph and EDX mapping for Si-80-Zr-20 catalyst granule.

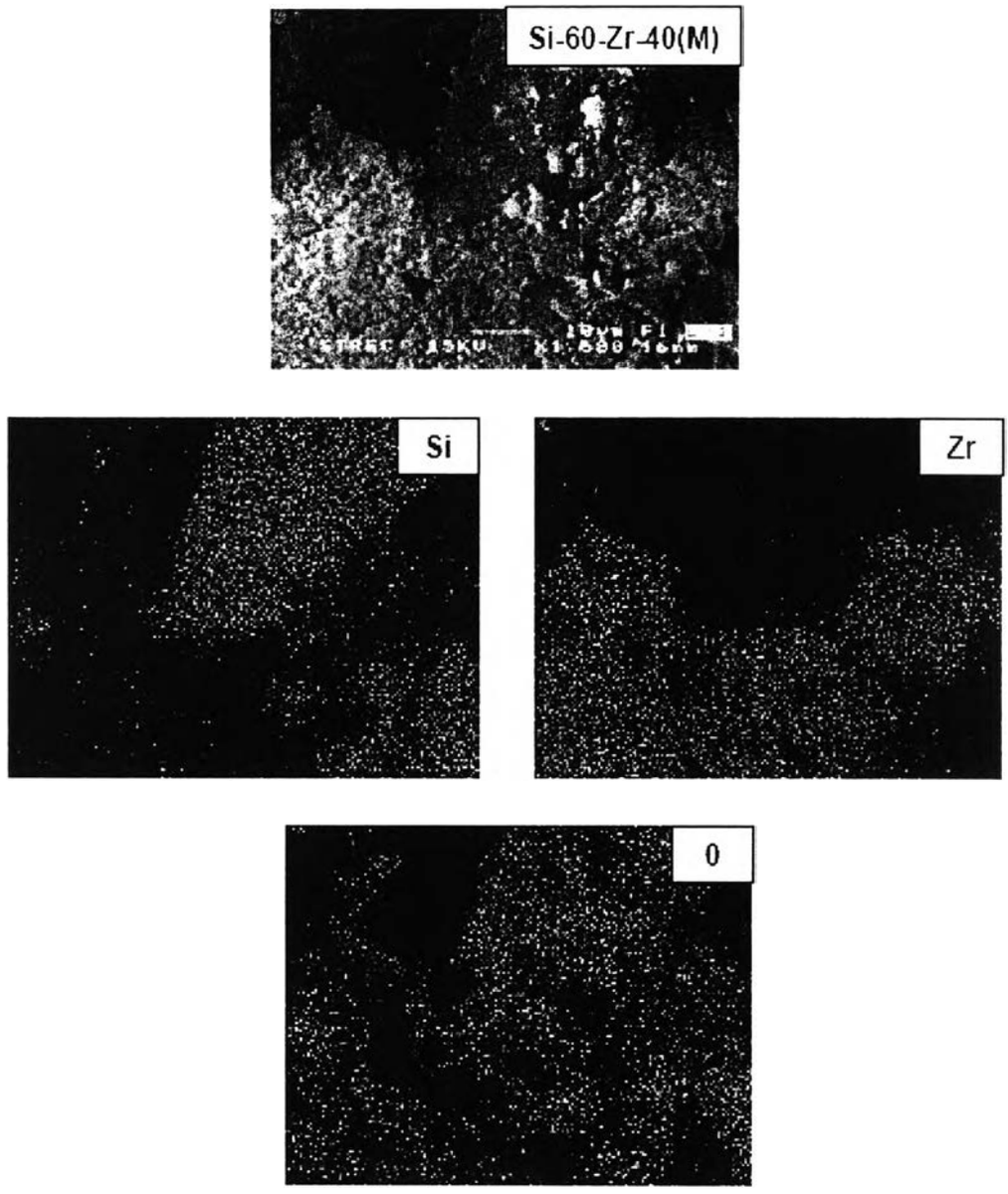

Figure 5.19 SEM micrograph and EDX mapping for Si-60-Zr-40 catalyst granule.

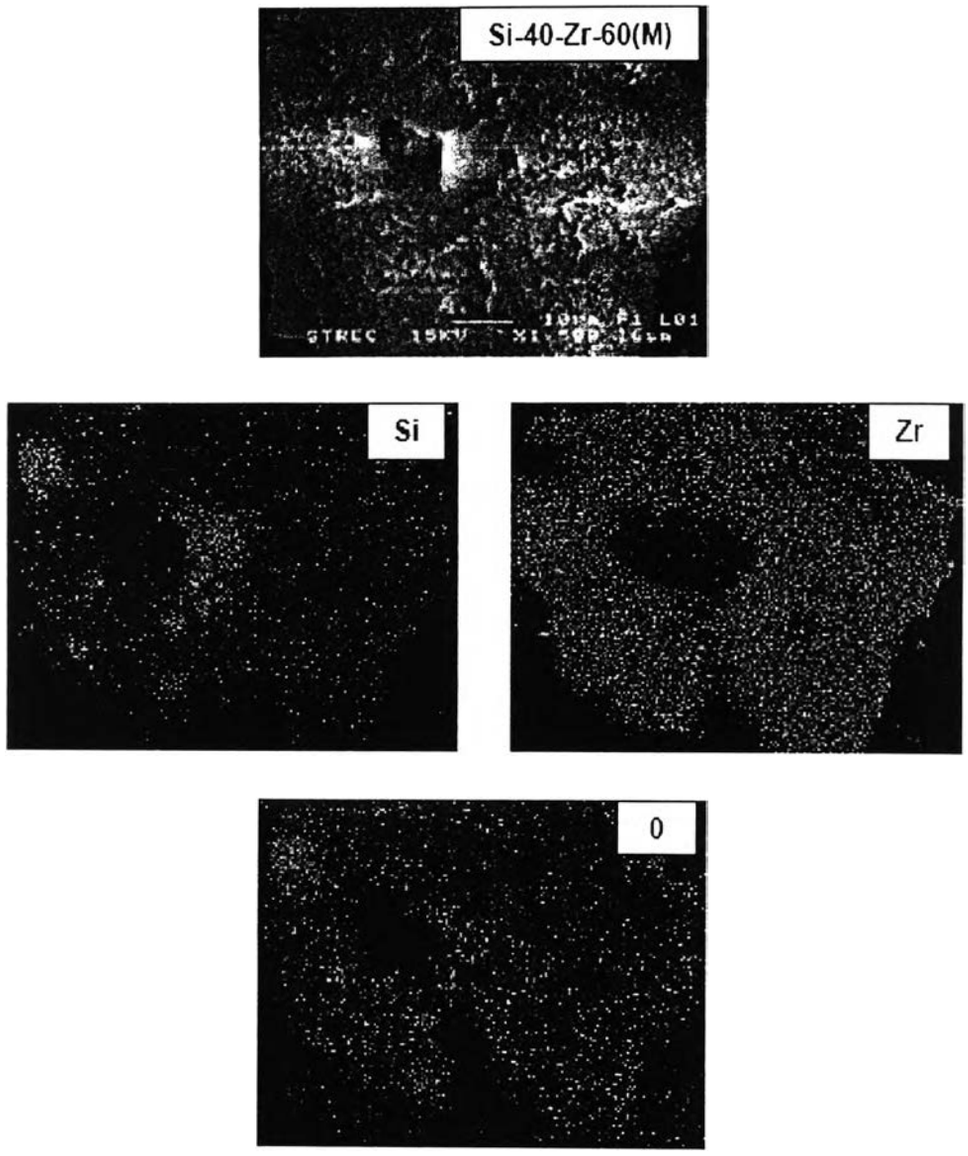

Figure 5.20 SEM micrograph and EDX mapping for Si-40-Zr-60 catalyst granule.

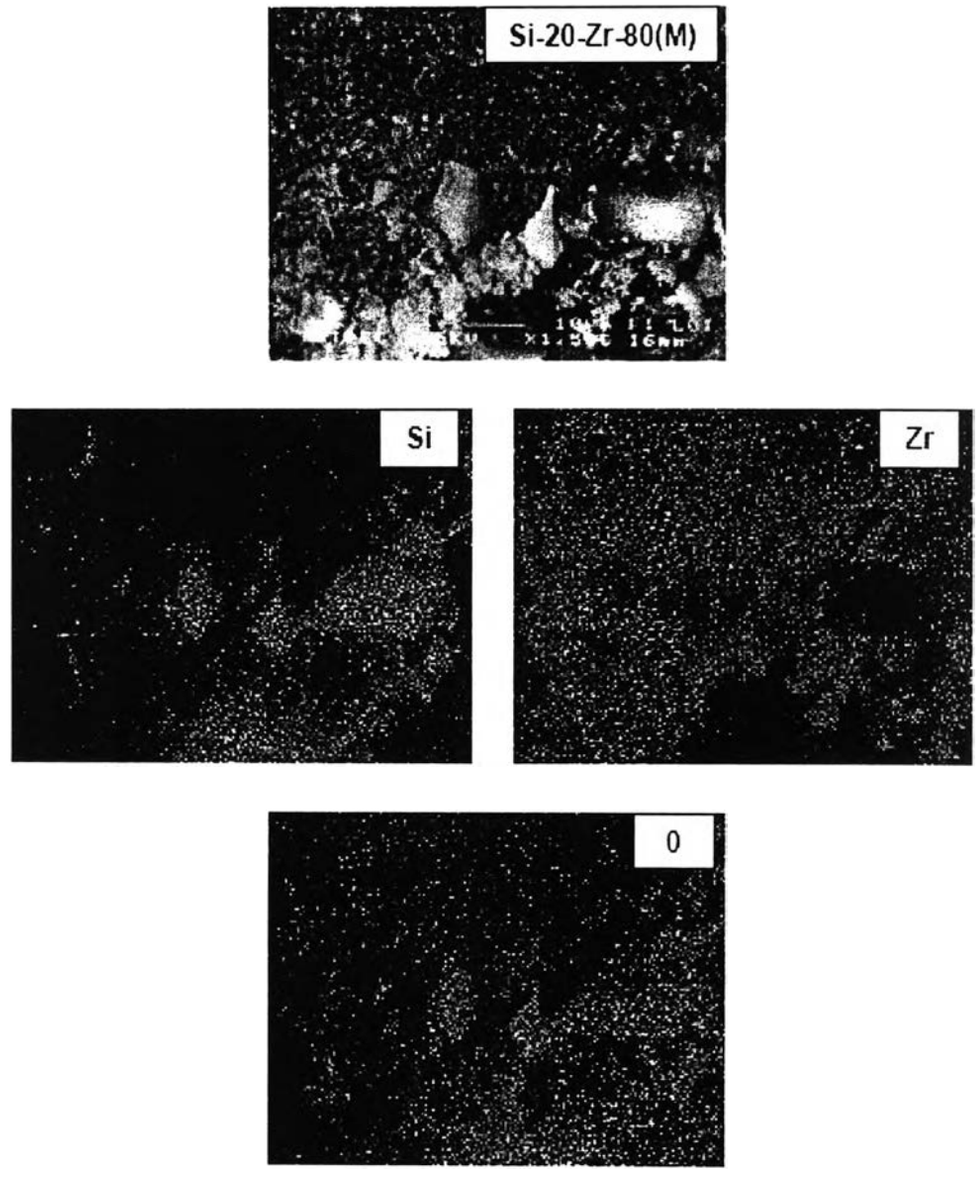

Figure 5.21 SEM micrograph and EDX mapping for Si-20-Zr-80 catalyst granule.

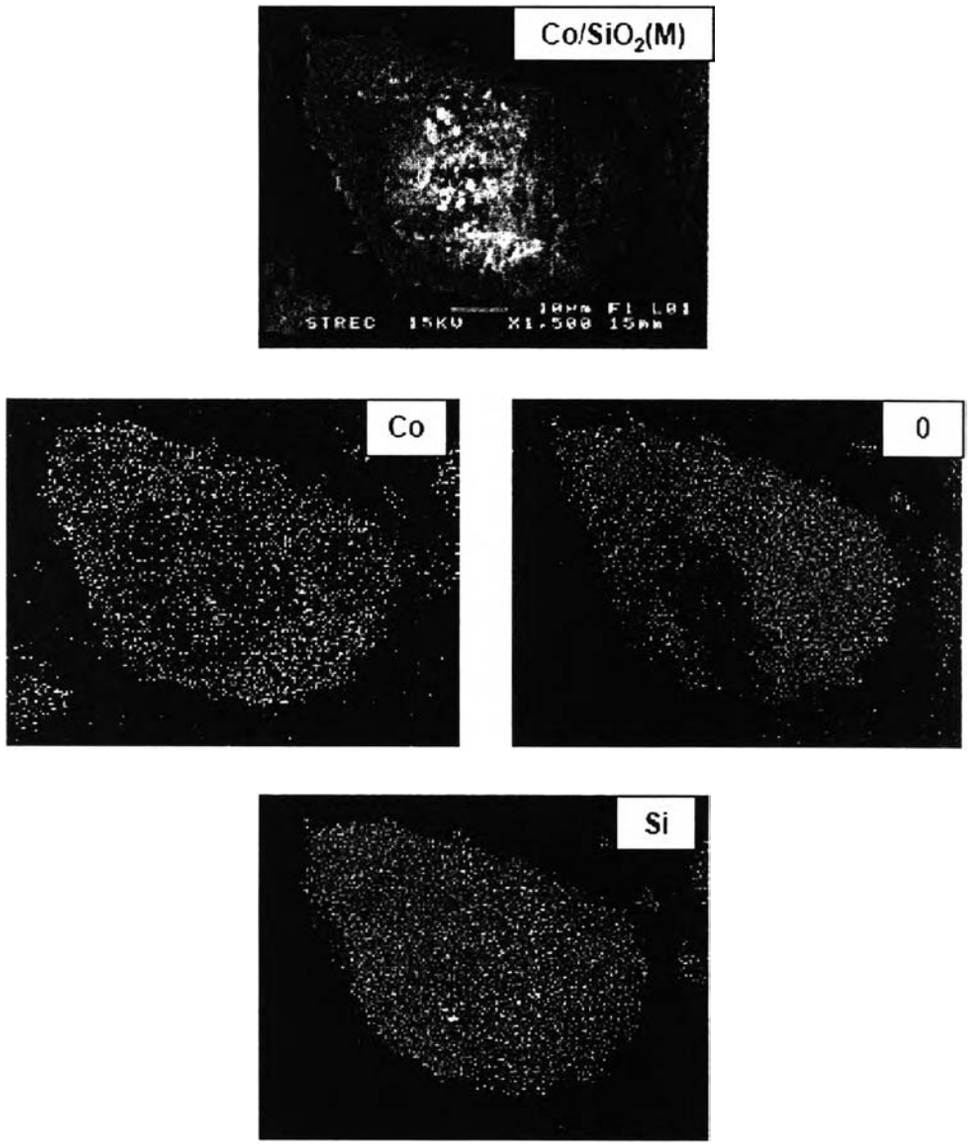

Figure 5.22 SEM micrograph and EDX mapping for Co/SiO_2 catalyst granule.

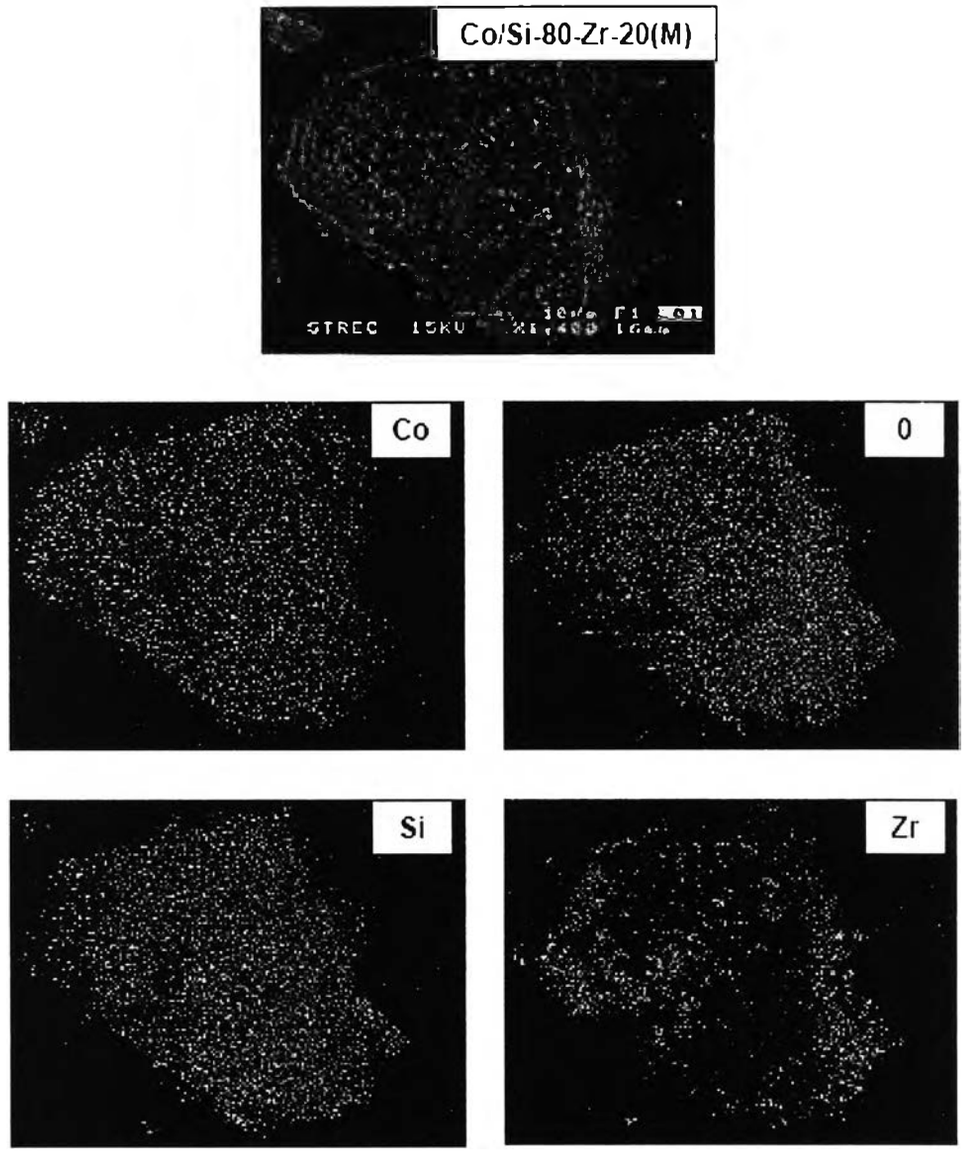

Figure 5.23 SEM micrograph and EDX mapping for Co/Si-80-Zr-20 catalyst granule.

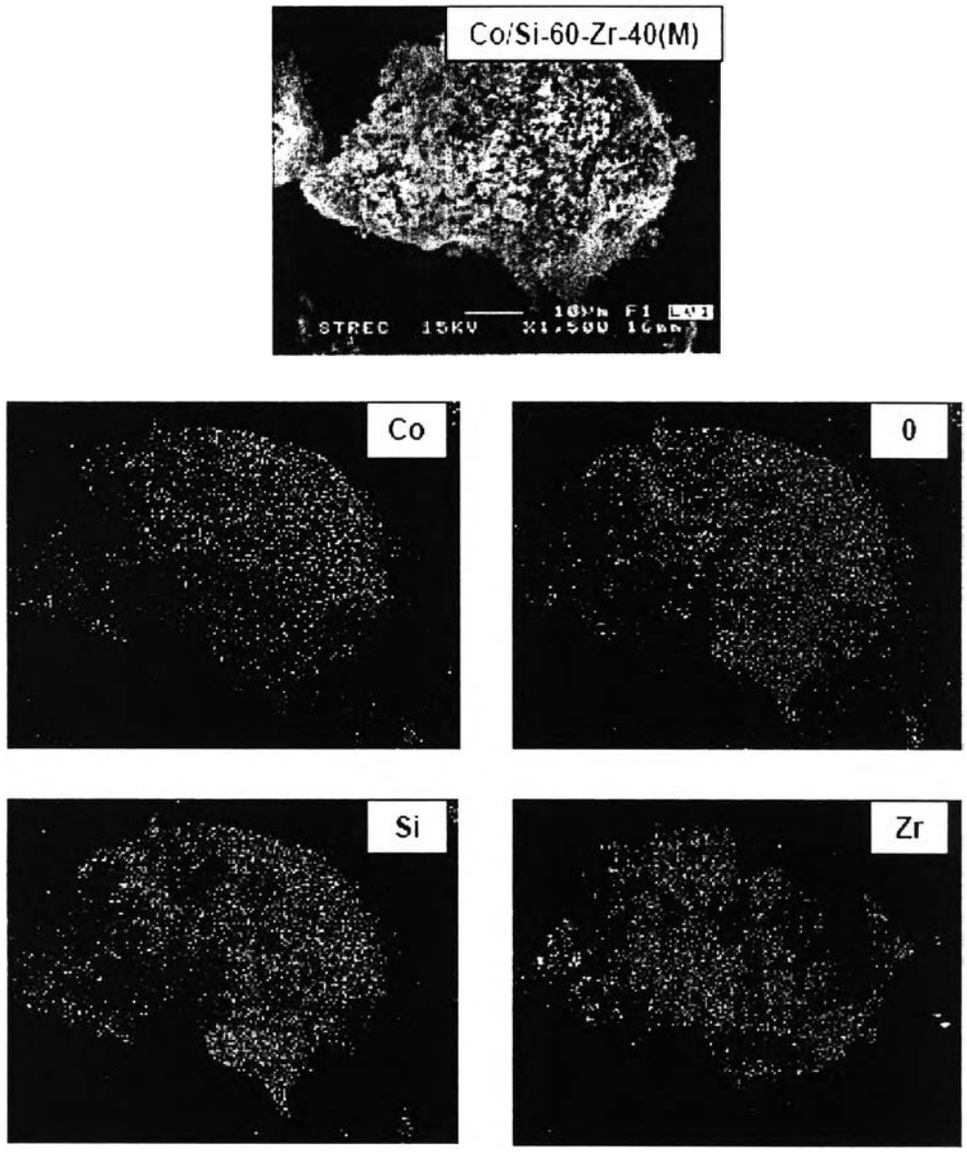

Figure 5.24 SEM micrograph and EDX mapping for Co/Si-60-Zr-40 catalyst granule.

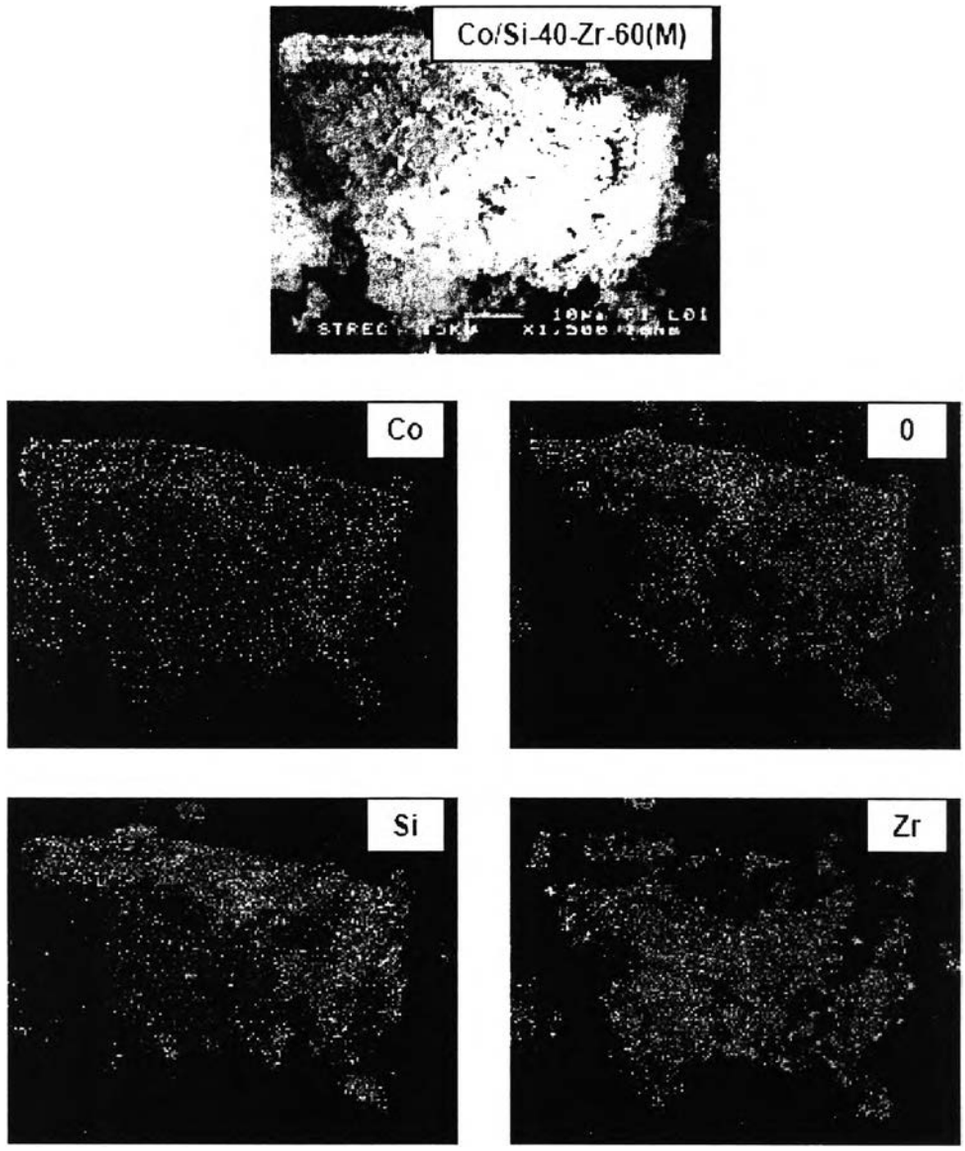

Figure 5.25 SEM micrograph and EDX mapping for Co/Si-40-Zr-60 catalyst granule.

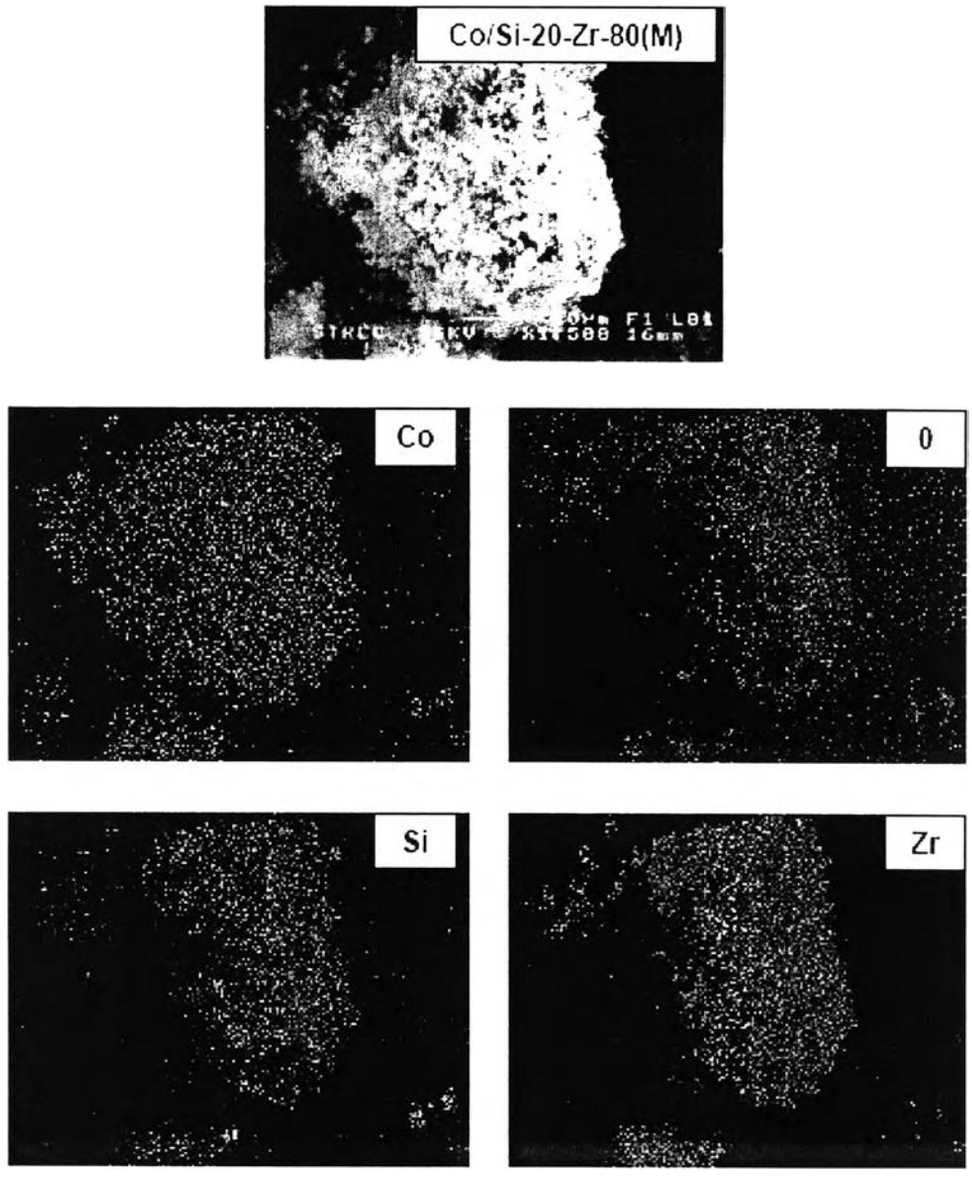

Figure 5.26 SEM micrograph and EDX mapping for Co/Si-20-Zr-80 catalyst granule.

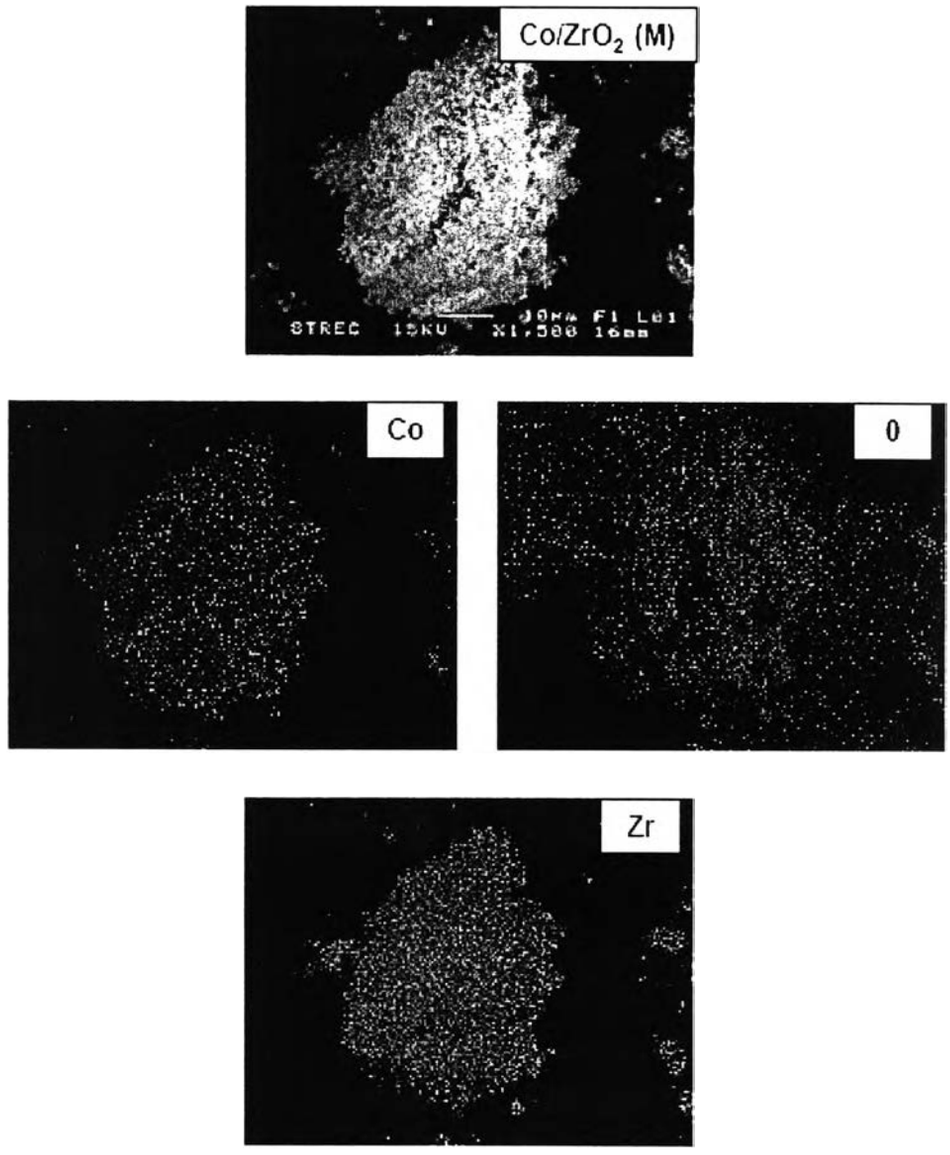

Figure 5.27 SEM micrograph and EDX mapping for Co/ZrO_2 catalyst granule.

5.2.4 Transmission Electron Microscopy (TEM)

TEM was conducted in order to identify the crystallite size and dispersion of Co oxide species on the various supports. The TEM micrographs for the micronscale supports and the Co oxide species dispersed on the various micronscale supports are shown in **Figures 5.28 and 5.30**, respectively. As seen in **Figure 5.28**, the amorphous micronscale SiO_2 exhibited only a dense of dark patches of SiO_2 whereas for the pure micronscale ZrO_2, it can be observed the single crystal of ZrO_2 in the micron size (more than 100 nm in diameter) seen as dark spots. For the mixed supports, the observation of ZrO_2 was predominant. The typical TEM micrograph of the mixed micronscale SiO_2-ZrO_2 is also shown [only for Si-40-Zr-60 (M)]. The dispersion of Co oxide species on the various micronscale supports is shown in **Figure 5.30**. In fact, it revealed the similar dispersion of Co for all various supports here. Although it can not differentiate the Co oxide species and ZrO_2, it indicated that Co oxide species dispersed on the micronscale supports were apparently in the micron size as well. Considering the TEM micrographs for the nanoscale supports and the Co oxide dispersed on the various nanoscale supports, they are illustrated as seen in **Figures 5.29 and 5.31**, respectively. The similarity for the micron- and nanoscale SiO_2 can be observed. However, the difference in TEM micrographs for the micron- and nanoscale ZrO_2 was evident. Obviously, the nanoscale ZrO_2 appeared in the smaller crystal in the nano size (~35-40 nm). TEM micrographs of the mixed nanoscale supports also exhibited the similar appearance with those from the nanoscale ZrO_2. The typical TEM micrograph [Si-40-Zr-60 (N)] for the mixed nanoscale supports is also shown in **Figure 5.29**. The TEM micrographs for Co oxide species dispersed on the various nanoscale supports (**Figure 5.31**) showed very interesting results where good dispersion of Co oxide species can be achieved onto the nanoscale supports. This was suggested that the dispersion of Co oxide species could be altered with the size of the support used. On the other hand, the Co oxide species dispersing on the micronscale support were in the micron size whereas those were in the nano size on the nanoscale one. However, it should be noted that the highly dispersed forms of Co oxide species are not only the factor that insure large number of reduced cobalt metal surface atoms for the samples as reported in our previous work (B. Jongsomjit *et al.*, 2005). Besides the dispersion of Co oxide species, the

interaction between them and the support need to be further investigated. Therefore, the TPR measurement was performed for such the purpose.

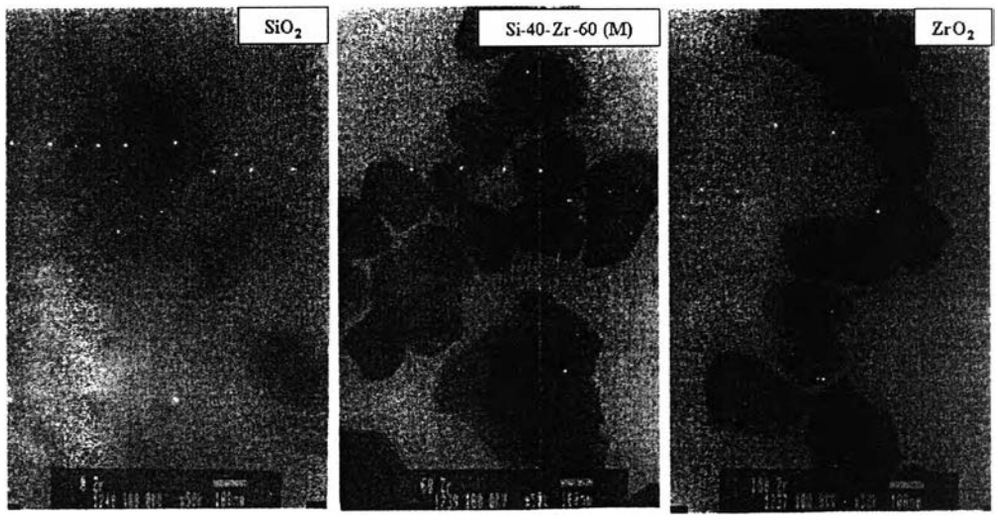

Figure 5.28 TEM micrographs of the micron-SiO_2, the micron-ZrO_2 and the mixed micron-SiO_2/ZrO_2 supports.

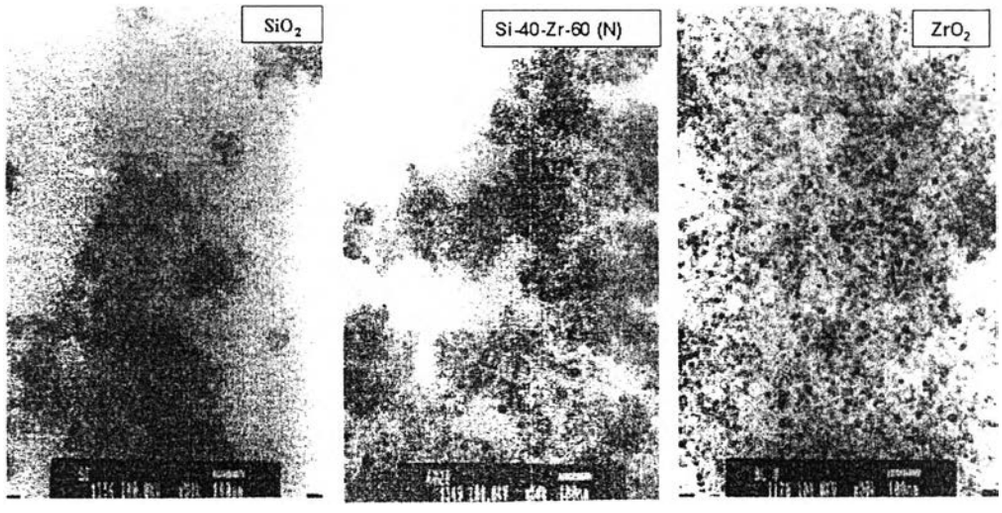

Figure 5.29 TEM micrographs of the nano-SiO_2, the nano-ZrO_2 and the mixed nano-SiO_2/ZrO_2 supports.

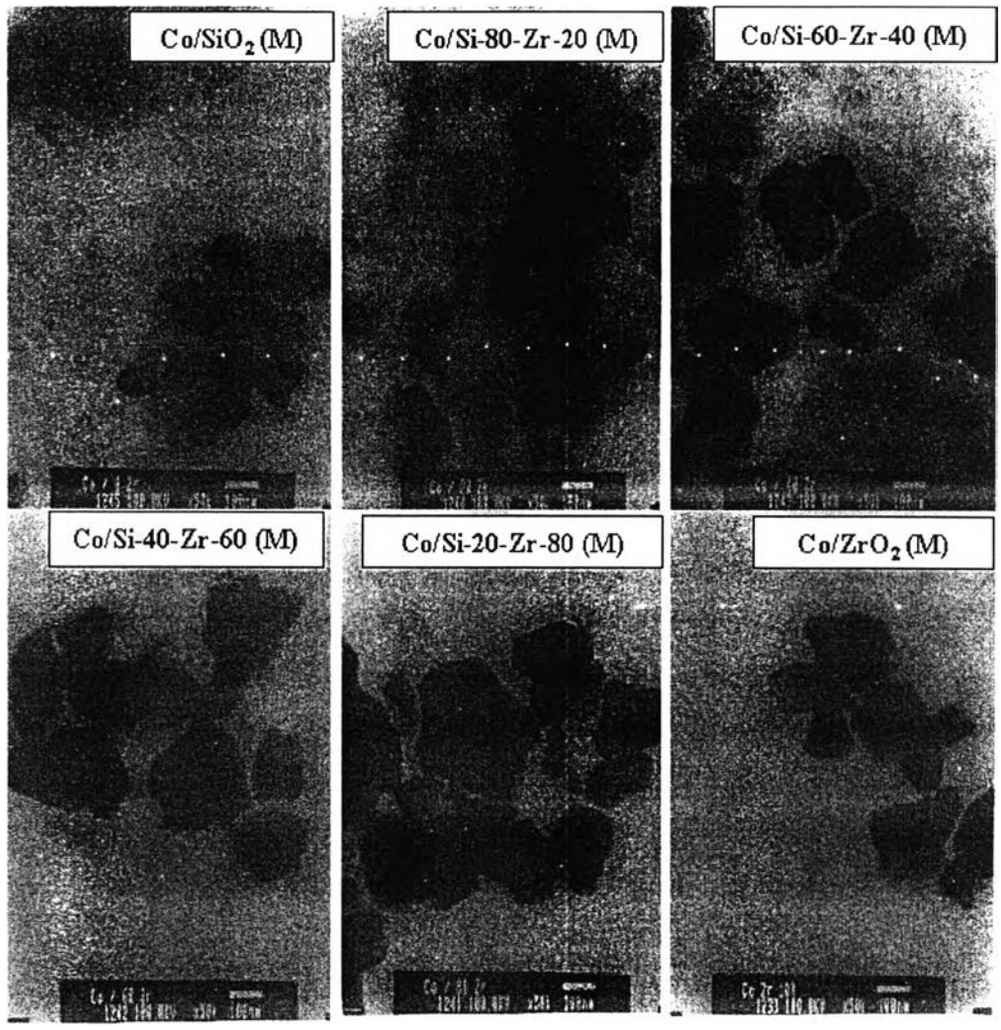

Figure 5.30 TEM micrographs for all cobalt dispersed on the various supports (micron).

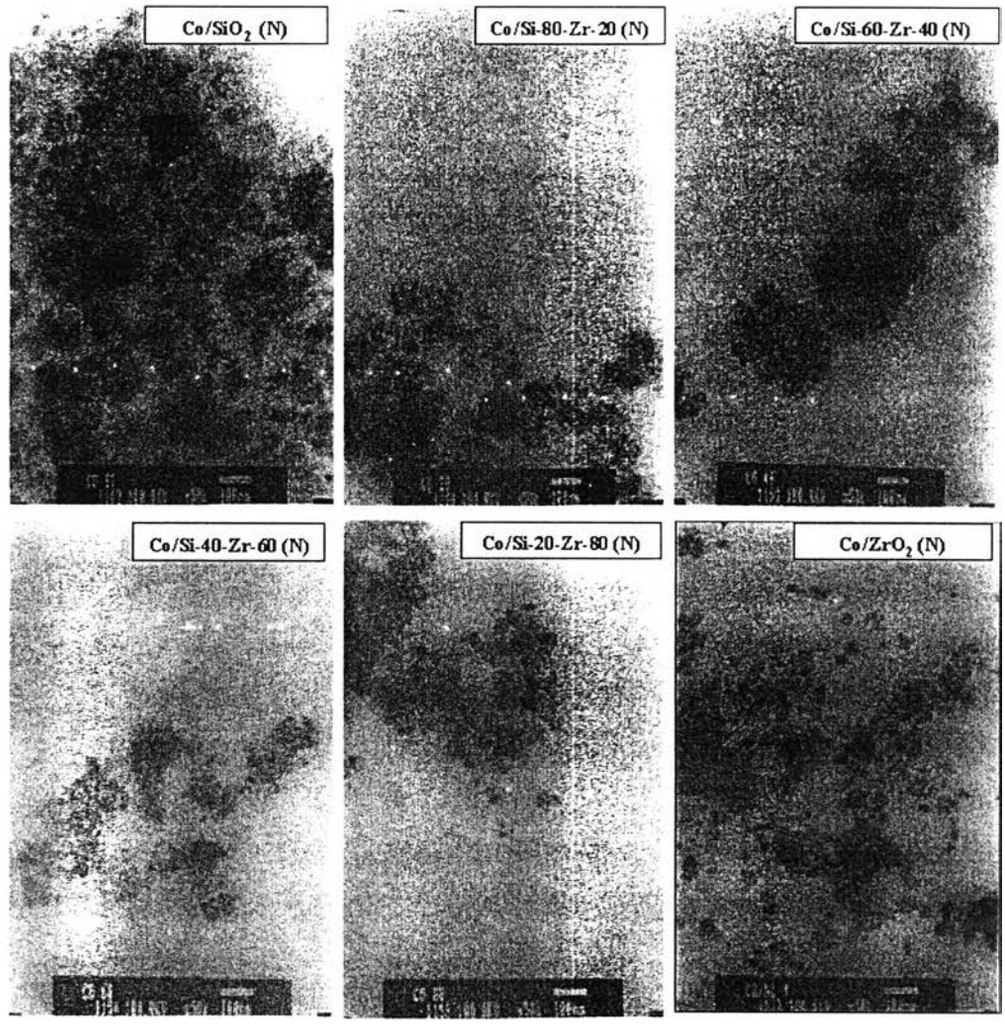

Figure 5.31 TEM micrographs for all cobalt dispersed on the various supports (nano).

5.2.5 Temperature programmed reduction (TPR)

TPR profiles of the Co catalysts on the various micron- and nanoscale supports are shown in **Figures 5.32 and 5.33**, respectively. As can be seen in **Figure 5.32**, there were two major reduction peaks located at ca. 320° and 420°C for the micronscale support. These peaks were related to the following step: Co_3O_4 to CoO, CoO to Co metal, and Co_XO_Y-support to Co metal, where Co_XO_Y-support was represented the Co oxide species strongly interacted with the support. In some cases, the peak of the decomposition of cobalt nitrates (as the precursor) during TPR of supported Co catalysts can be observed at temperatures between 200° to 300°C, especially with silica and alumina supports (B. Jongsomjit *et al.*, 2002). Prolonged calcination or reduction and recalcination resulted in completed decomposition of any cobalt nitrates present (B. Jongsomjit *et al.*, 2001). However, there was no observation of the decomposition peak of cobalt nitrate in this present study. Considering the TPR profiles of Co oxide species dispersed on the nanoscale supports as shown in **Figure 5.33**, there was only one major reduction peak located at ca. 440 to 470°C. Again this peak was also related to the reduction of Co_3O_4 to CoO, CoO to Co metal, and Co_XO_Y-support to Co metal as mentioned before. It should be noted that with using the nanoscale support, the interaction of Co oxide species was more homogeneous leading to only one reduction peak observed. In order to give a better understanding, the suggested reduction behaviors of Co oxide species on different micron- and nanoscale supports are shown in **Figures 5.34**.

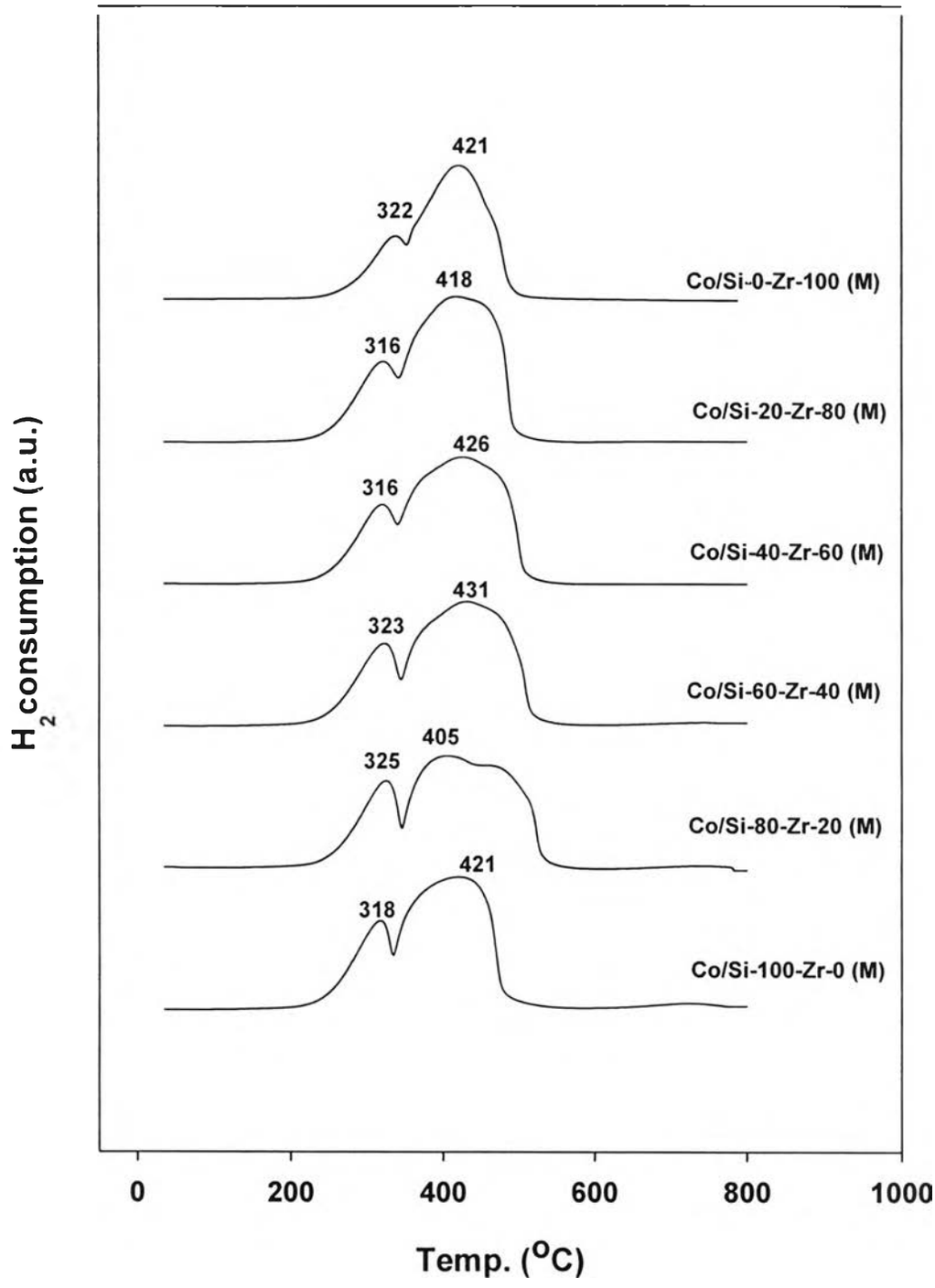

Figure 5.32 TPR profiles for the mixed micron- SiO_2/ZrO_2-supported Co catalyst.

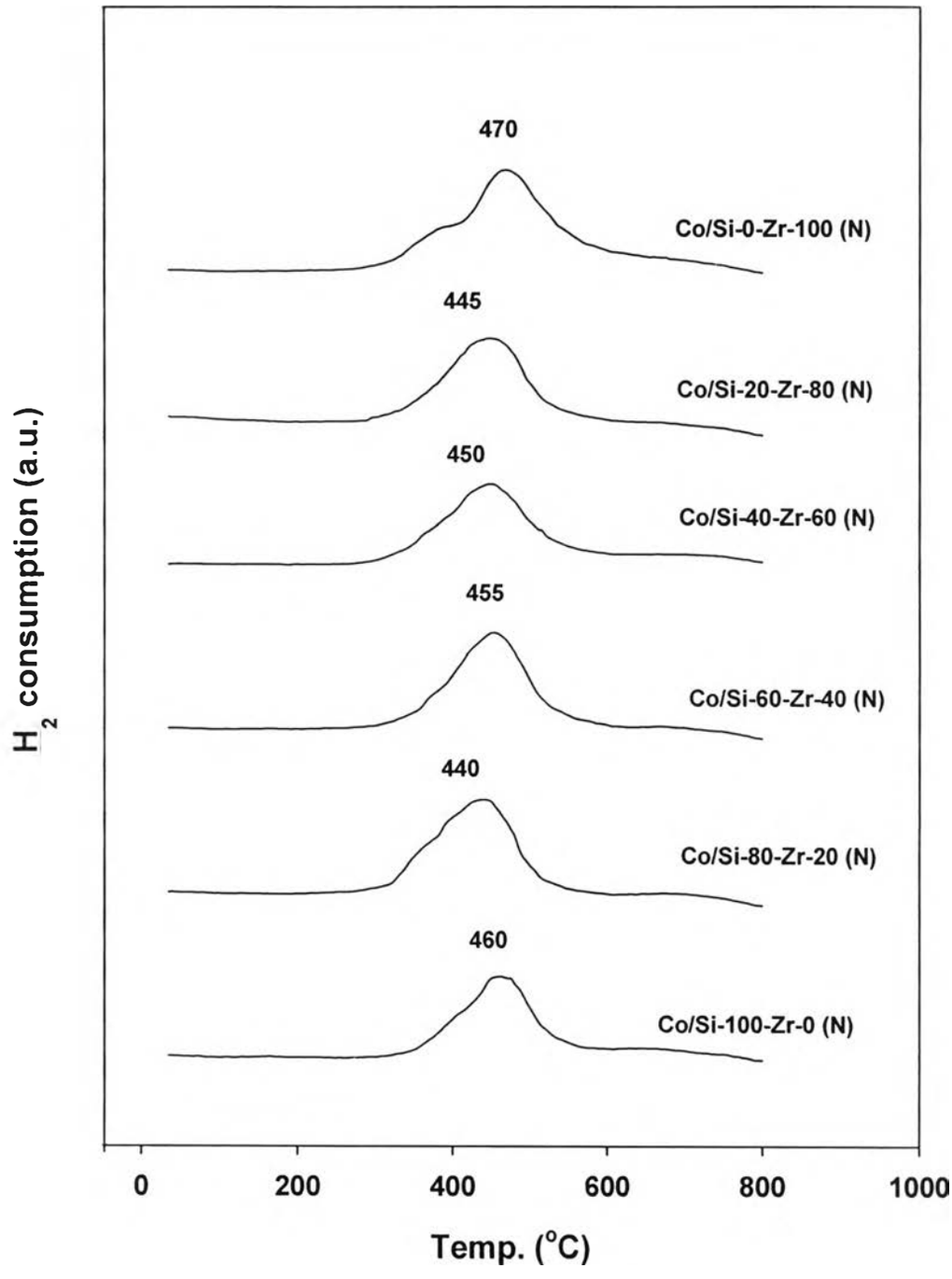

Figure 5.33 TPR profiles for the mixed nano- SiO_2/ZrO_2-supported Co catalyst.

Table 5.5 Initial and final temperature from TPR profiles for the mixed micron-SiO_2-ZrO_2-supported Cobalt catalyst

Catalyst samples	Temperature (°C)			
	Peak 1		Peak 2	
	Initial	Final	Initial	Final
Co/SiO_2 (M)	190	335	335	535
Co/Si-80-Zr-20 (M)	185	345	345	570
Co/Si-60-Zr-40 (M)	190	345	345	570
Co/Si-40-Zr-60 (M)	180	340	340	570
Co/Si-20-Zr-80 (M)	200	345	345	560
Co/ZrO_2(M)	200	350	350	555

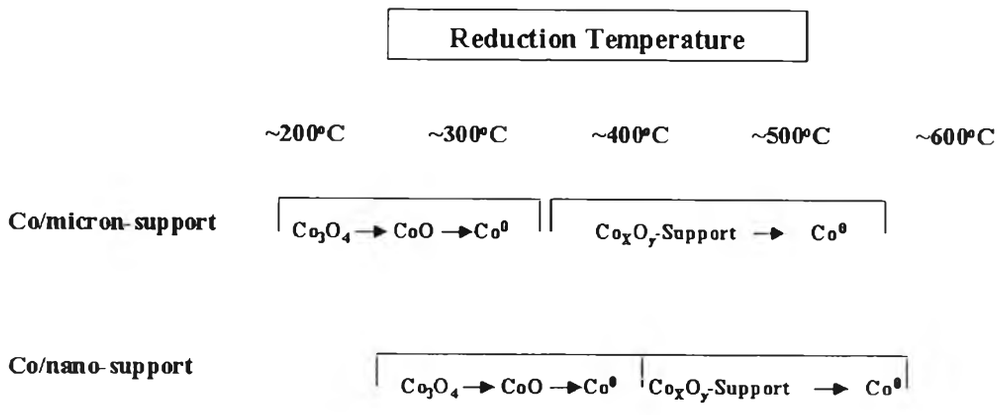

Figure 5.34 Schematic 0f reduction behaviors of Co oxide species on different micron- and nanoscale supports.

5.2.6 Reaction study in CO hydrogenation

CO hydrogenation was performed to measure the overall activity of the catalyst samples on various micron- and nanoscale mixed supports. The reaction rate and product selectivity during CO hydrogenation at steady-state are revealed in **Table 5.4**. For the Co catalysts on the pure SiO_2, it can be observed that the catalyst on the micronscale SiO_2 exhibited higher activity than that on the nanoscale SiO_2 support without any changes in the product selectivity. However, when the SiO_2 support was mixed with ZrO_2 for both micron- and nanoscale supports, the similar trend regarding to the activity and product selectivity as seen with the pure SiO_2 was still observed. It was suggested that the effect of SiO_2 was predominant compared to ZrO_2. Considering when the pure ZrO_2 support was used, the result was essentially opposite. It indicated that the catalyst on the nanoscale ZrO_2 exhibited higher activity than that on the micronscale ZrO_2 support. In addition, the selectivity to C_2-C_4 was slightly higher with the ZrO_2 support. These results based on the ZrO_2 support were in accordance with those reported by Panpranot *et al.*. The increased activity for the nanoscale ZrO_2 support can be attributed to the larger number of reduced Co metal surface atoms. Since CO hydrogenation is a structure insensitive reaction, thus, the catalytic activity depends only on the number of reduced Co metal surface atoms available for catalyzing the reaction. In particular, differences in the catalytic performance based on using the micron- and nanoscale SiO_2 and ZrO_2 supports can be described by the reduction behaviors of the catalysts on various supports. TPR peak locations are affected by reduction kinetics. A wide range of variables including particle size, support interaction and the reduction gas composition (B. Jongsomjit *et al.*, 2002) can affect the kinetics of reduction. The effects of particle size and support interaction can be superimposed on each other. Thus, while a decrease in metal oxide particle size can result in faster reduction due to a greater surface area/volume ratio, smaller particles may interact more with the support, slowing reduction. In order to give a better point of view, **Figure 5.35** is present here. As mentioned, the particle size and support interaction effects can be perhaps divided into two categories as shown in **Figure 5.35**. As seen in **Figure 5.35(a)**, the difficulty of reduction for the catalyst and support with strong interaction increases with decreased particle size. In contrast, with weak interaction between the catalyst and support, the difficulty of reduction increased with increased particle size as shown in

Figure 5.35(b). Based on the resulted activities, it can be concluded that for SiO_2, the **Figure 5.35(a)** can be used due to the fact that SiO_2 strongly interacted with the Co oxide species. Hence, the Co catalysts on the micronscale SiO_2 were more active. On contrary, **Figure 5.35(b)** can be applied for the Co oxide species on the ZrO_2. With weak interaction between the catalysts on the nanoscale ZrO_2 were more active. This indicates that besides the support interaction and particle size, the nature of different supports is also the key to determine how active the catalyst is.

Table 5.6 Reaction rate and product selectivity during CO hydrogenation.

Sample	Reaction Rate (x 10^2 gCH_2/g cat. h)		Product Selectivity (%)			
			C1		C2-C4	
	N	M	N	M	N	M
Co/SiO_2	29.9	37.5	99.5	99.2	0.5	0.8
Co/Si-80-Zr-20	21.6	37.3	98.7	99.5	1.3	0.5
Co/Si-60-Zr-40	12.3	37.4	98.0	99.4	2.0	0.6
Co/Si-40-Zr-60	28.0	37.3	99.1	99.6	0.9	0.4
Co/Si-20-Zr-80	25.2	35.5	99.1	99.4	0.9	0.6
Co/ZrO_2	25.3	5.3	96.3	95.8	3.7	4.2

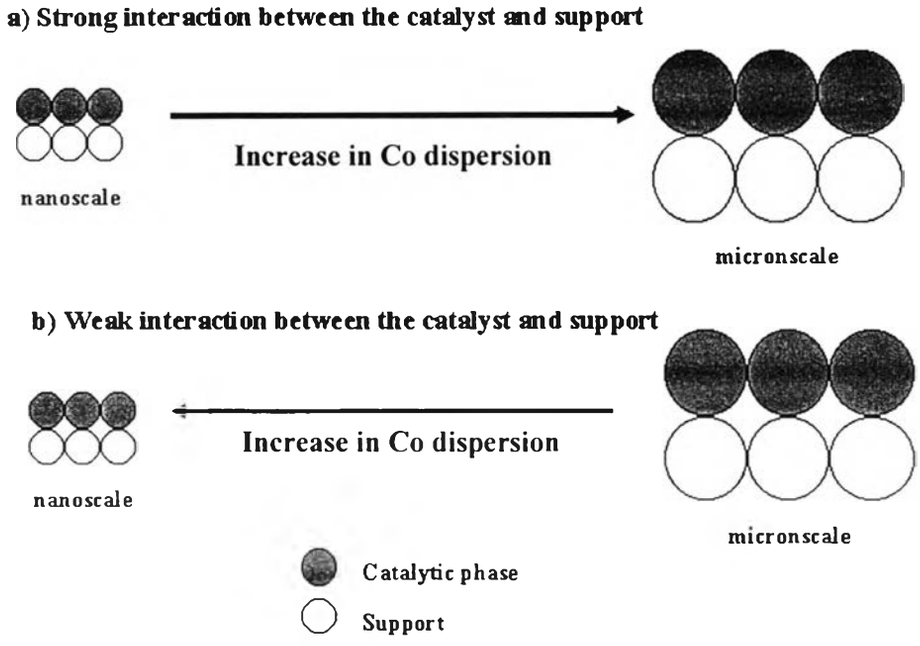

Figure 5.35 Schematic of the effects of particle size and support interaction.